

2011
2012

GENEESKUNDE

*master in de biomedische wetenschappen: bio-elektronica
en nanotechnologie*

Masterproef

*Detection of DNA-Hybridization Using Interdigitated
Electrodes Functionalized with Graphene*

Promotor :
Prof. dr. Patrick WAGNER

Promotor :
prof. dr. SVEN INGEBRANDT

Ruben Lanche

*Masterproef voorgedragen tot het bekomen van de graad van master in de biomedische
wetenschappen , afstudeerrichting bio-elektronica en nanotechnologie*

De transnationale Universiteit Limburg is een uniek samenwerkingsverband van twee universiteiten in twee landen:
de Universiteit Hasselt en Maastricht University

universiteit
hasselt
KNOWLEDGE IN ACTION

 Maastricht University

Universiteit Hasselt | Campus Diepenbeek | Agoralaan Gebouw D | BE-3590 Diepenbeek
Universiteit Hasselt | Campus Hasselt | Martelarenlaan 42 | BE-3500 Hasselt

 Maastricht University

universiteit
hasselt
KNOWLEDGE IN ACTION

2011
2012

GENEESKUNDE

*master in de biomedische wetenschappen: bio-elektronica
en nanotechnologie*

Masterproef

*Detection of DNA-Hybridization Using Interdigitated
Electrodes Functionalized with Graphene*

Promotor :
Prof. dr. Patrick WAGNER

Promotor :
prof. dr. SVEN INGEBRANDT

Ruben Lanche

*Masterproef voorgedragen tot het bekomen van de graad van master in de biomedische
wetenschappen , afstudeerrichting bio-elektronica en nanotechnologie*

Table of Contents

Abbreviations.....	3
Acknowledgements	5
Abstract.....	7
1. Introduction.....	9
1.1. State of the art and motivation.....	9
1.1.1. Graphene based DNA sensing.....	12
1.2. Objective of this thesis	13
1.3 Fundamentals.....	13
1.3.1 Graphene's properties	13
1.3.2 Impedance Spectroscopy (IS).....	14
1.3.3 Interdigitated electrodes (IDEs).....	15
2. Materials and methods.....	17
2.1. DNA sensor fabrication.....	17
2.1.1. Design of shadow mask for fabrication of IDEs.....	17
2.1.2. GO deposition and Dielectrophoresis (DEP).....	18
2.1.3. Reduction of GO by L-Ascorbic acid (L-AA)	20
2.1.4. DNA immobilization.....	21
2.1.5. DNA Hybridization-Denaturation.....	21
2.3. Characterization.....	22
2.3.1) Scanning electron microscope (SEM).....	22

2.3.2) Atomic force microscope (AFM).....	23
3) Results and discussion	25
3.1) GO solution.....	25
3.2) DEP deposition of GO and rGO.....	25
3.2.1) Physical characterization.....	25
3.2.2) Electrical characterization.....	31
3.3) DNA sensor.....	34
3.3.1) Physical characterization	34
3.3.2) Electrical characterization	34
4) Conclusions and outlook.....	41
References.....	43
Supplementary section.....	45
Part 1: IS measurements.....	45
Part 2: Chip fabrication protocol.....	54
Part 3: Measurement cell design.....	56

Abbreviations

AFM :	Atomic Force Microscope
AC :	Alternating Current
cDNA :	Complementary DNA
DEP:	Dielectrophoresis
DI:	Deionized
DNA:	Deoxyribonucleic Acid
dsDNA :	Double Stranded DNA
EDC:	1-ethyl-3-[3-dimethylaminopropyl]-carbodiimide
IDEs:	Interdigitated Electrodes
IS :	Impedance Spectroscopy
GO:	Graphene Oxide
KH ₂ PO ₄ :	Monopotassium phosphate
L-AA:	L-Ascorbic Acid
MES:	2-[N-morpholino]-ethanesulphonic acid
NaCl:	Sodium Chloride
Na ₂ HPO ₄ ·2H ₂ O:	Disodium phosphate dihydrate
NaOH:	Sodium Hydroxide
PBS :	Phosphate Buffered Saline
RC:	Resistive Capacitive
rGO:	reduced Graphene Oxide

RT :	Room Temperature
SDS :	Sodium Dodecyl Sulphate
Si :	Silicon
SiO ₂ :	Silicon Oxide
SSC :	Saline Sodium Citrate
ssDNA:	single stranded DNA
sulfo-NHS:	N-hydroxysulfosuccinimide

Acknowledgments

I would like to thank Prof. Dr. Sven Ingebrandt (Biomedical Signalling Group, Informatics & Microsystem Technology) and Prof. Dr. Patrick Wagner (Institute for Materials Research, Hasselt University) for allowing me to do my thesis in such an exciting and novel topic in the department of Informatics and Microsystems Technology in the Fachhochschule Kaiserslautern.

The Biomedical Signalling group in FH KL for considering me a part of the group as well as for their help and especially Dr. Xuan Thang Vu for his advice regarding IS measurements.

My thanks to Erik Engelman, Peter Molter, Rainer Lilischkis, Lothar Greiner, Detlev Cassel, Petra Boeswald and Heike Mueller for their technical support at all times.

Tanya Jacobs for teaching me how to pour a Trappist and also for reading and commenting on my written thesis.

Lotta Delle for being my translator, lab partner and especially my friend, making me feel less of a stranger in a strange land.

My family for their support and especially my sister Lucia Lanche for economic support and hopefully low interest rates.

Lastly I would like to thank Dr. rer. nat. Maryam Weil, my Jedi master. Without whose direction and guidance through every step of the process, this thesis would have never seen the light.

Abstract

Label-free detection of DNA hybridization and denaturation events using interdigitated electrodes (IDEs) is one of the most attractive approaches for a new generation of biochips with direct electrical readout for a fast, simple and cost-effective analysis.

Recently, graphene-based biosensors have been used for impedimetric detection of DNA. The novel nanomaterial graphene, with its excellent electrical properties and biocompatibility, has significantly improved the impedimetric sensor characteristics. In this study, an array of IDEs functionalized with reduced graphene oxide (rGO) was developed. This platform has been used for the impedimetric-detection of DNA hybridization and denaturation.

An array of four Au-IDEs was fabricated on Si/SiO₂ (300 nm SiO₂) and glass substrates. The active area of the fabricated IDEs has been functionalized with a GO layer using dielectrophoresis (DEP). The GO layer was reduced using L-Ascorbic Acid (L-AA). Finally, the surface of each rGO-IDE was functionalized with single-stranded DNA (ssDNA) molecules with perfectly matched or fully mismatched DNA-sequences to that of the complementary ssDNA (cDNA) molecules.

For detection of the DNA hybridization and denaturation, the developed DNA-chip was mounted in a measurement cell and characterized by impedance spectroscopy (IS). The DNA hybridization and denaturation experiments were carried out in a differential IS setup using an impedance analyzer to eliminate the effect of disturbing factors (e.g. temperature) in the sensor's signal.

Changes in impedance for the sensors functionalized with perfect-matched ssDNA after a hybridization event were observed in contrast to almost no change when fully miss-matched ssDNA was used.

1. Introduction

1.1. State of the art and motivation

It is hard to believe that a material like graphene, has spiked so much interest in so little time. However, when the unique mechanical, electrical, chemical, structural and optical properties of this planar sheet of sp^2 -bonded carbon atoms with one atom thickness are taken into account, it becomes a little easier to process. The number of publications and research invested in this novel nanomaterial has surpassed its fellow carbon materials such as fullerenes or carbon nanotubes. Starting in 2004 when it was first mechanically exfoliated and highly impulsed by the 2010 Nobel prize, graphene is definitely a material worth looking further into^[1,2].

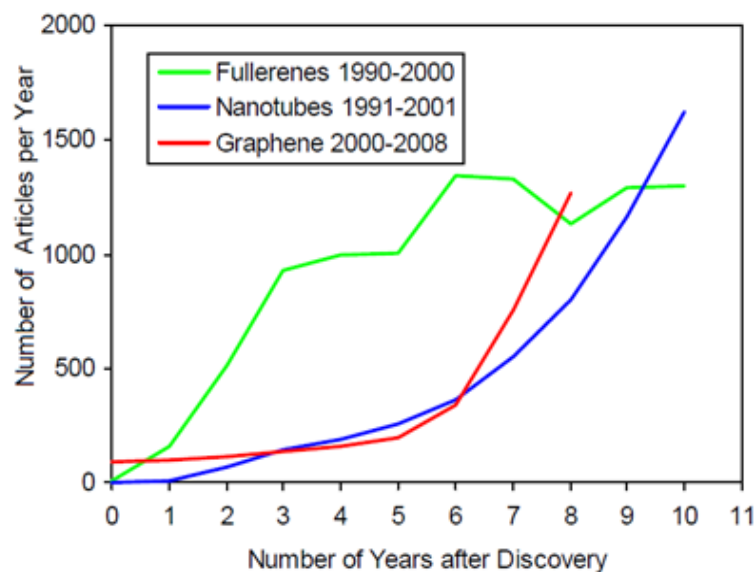


Fig. 1.1 Number of articles since carbon allotrope discovery^[1].

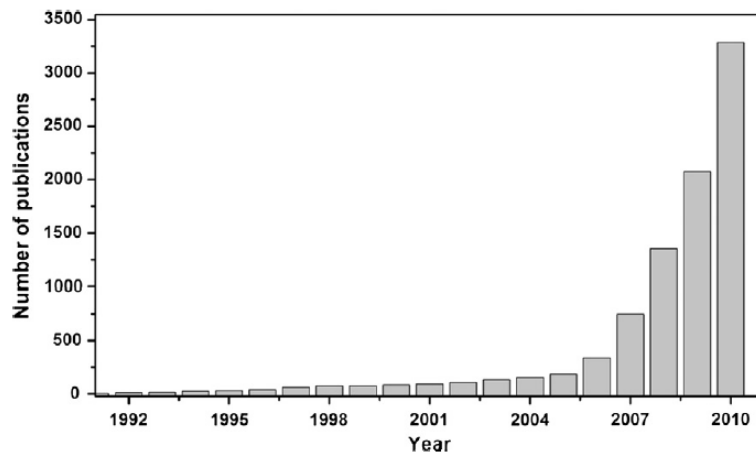


Fig. 1.2 Publications of graphene per year^[2].

Although the fabrication of pristine graphene sheets is still a process that needs to be optimized, there is nonetheless a great amount of research in several state-of-the-art applications regarding each of the materials extraordinary properties.

Graphene based transistors display an increased functioning speed compared to silicon samples due to the extremely high electron mobility at room temperatures^[3]. The electrons can actually travel for several micrometers without any scattering as if they had no mass. One of the big problems in moving the material from the lab to the electronic industry is its lack of bandgap, without which it is so far impossible to create a switching device with properties comparable to silicon devices. The analog electronics however uses a wide range of values, not only zero and one. Research is ongoing in this field where a single graphene device could take the place of 20 silicon transistors, reducing time and power consumption^[3].

Another interesting application of graphene is in bionic technology, owing to the fact that it can electrically interact with neurons and other cells communicating by electric potentials or pulses and because the material is unaffected by the ionic solutions in the human body. The flexibility of graphene has made it a perfect candidate for use in ear, eye and brain implants, since it can be wrapped around these tissues^[4].

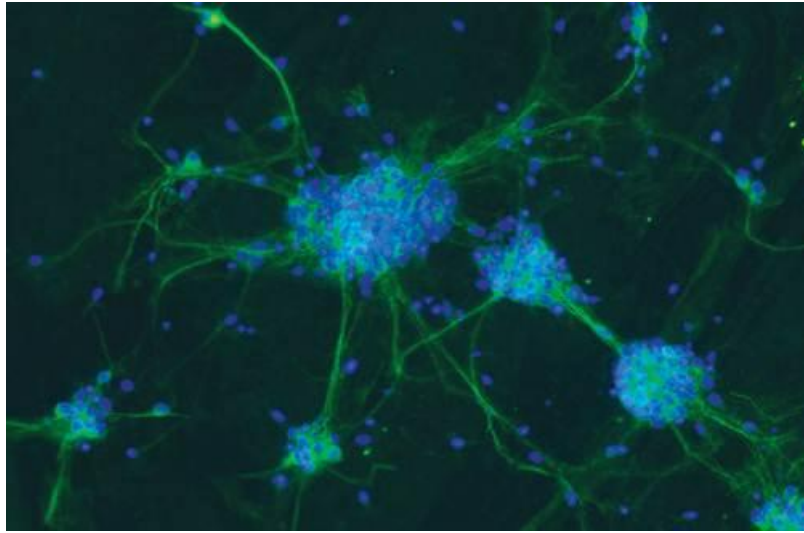


Fig. 1.3 Cortical neurons being grown on graphene for use as biological implants (nuclei are stained blue)^[4].

Photonics is another field where graphene is expected to make a big impact. Its transparency makes it useful for touchscreen or solar panel applications, its strength and flexibility but especially its low cost could change the way everyday products such as smart phones are known. Having the same light absorption throughout the entire electromagnetic spectrum, graphene gives rise to devices which could detect and emit terahertz radiation, a gap in the spectrum that has not been exploited. Graphene modulators could be installed in computer chips replacing copper wires with light beams for optical intercommunications, improving the speed of the devices^[5].

Although most of the hype comes from graphene's electrical properties, its chemical counterparts offer very interesting possibilities. If a continuous sheet of saddle shaped 'nano-foams' could be made, the fabrication of electrodes in very high energy-density and ultrafast super capacitors would become a reality, by far outperforming the existing devices. Using graphene's chemical properties as a reactant instead of a product, new paths of material processing could open up. Furthermore, changes in graphene's morphology make it theoretically possible to tune its chemical activity^[6]. And most of all, because of its low cost and low environmental impact it is considered an ideal material for the construction of different biosensors and biotransducers.

1.1.1 Graphene based DNA sensing

A biosensor is defined as a tool or system composed of biological material immobilized as a recognition element on its substrate (Fig. 1.4). The chosen biological material is in contact with a transducer which translates the biochemical signal into a measurable electrical signal. The selection of the biological component will of course depend on the substance to be analyzed. Quality of human life in general can be greatly improved by biosensing. They provide a selective, sensitive and cheap detection method to a vast amount of compounds for use in health care ^[7]. The rapid growth of higher age groups in first world countries has drawn special attention to the investment in new methods for point of care analysis of diseases, therefore fast and sensitive DNA analysis has become extremely important in clinical diagnosis. Technologies in DNA biosensing^[30] have special appeal not only for their low cost and simplicity but ultimately for their capabilities in detecting single nucleotide polymorphisms which have been correlated to diseases and genetic disorders such as Alzheimer's and Parkinson's disease^[8].

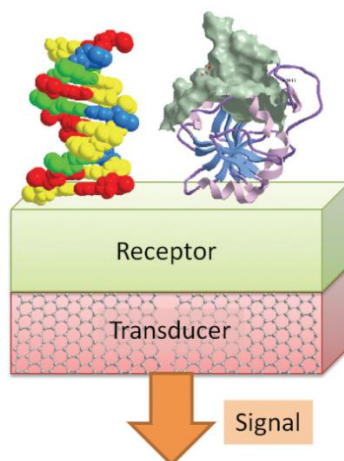


Fig. 1.4 Scheme of a biosensor. The biosensor consists of a receptor layer, which consists of a biomolecule (e.g., DNA or protein), and a transducer, which is a graphene-based material^[7].

On graphite only adenine (A) and guanine (G) give useful analytical signals which is not the case for cytosine (C) and thymine (T), due to their signals being smaller. The high defect density of chemically rGO provides well resolved signals for all DNA bases, A,G,C and T because of their different oxidation

potentials, making it ideal as a transducer in a DNA label free biosensor^[9,10]. Gold nanoparticles (AuNPs) and other metal nanoparticles have also been used in order to enhance the sensitivity of these sensors^[7,11,12,13].

1.2 Objective of this thesis

In the present work the construction of a DNA sensor based on rGO functionalized IDEs will be described. The scope will include the description of the fabrication as well as the characterization of the biosensor. A green approach with L-ascorbic acid (L-AA) has been chosen for the method of reduction and dielectrophoresis was the method for rGO functionalization of the IDEs. Through physical and electrical characterization techniques the viability of the DNA sensor will be assessed.

1.3 Fundamentals

1.3.1 Graphene's properties

Pristine graphene is a semi-metal material with zero energy band-gap which makes it extremely useful in electrochemical sensing. The first way in which this material was obtained was by mechanical cleavage from graphite, it can also be grown on transition metal substrates or obtained by decomposing silicon carbide at high temperatures^[12]. It is however not so easy to work with. A solution to this problem has been to work with GO which is water soluble and therefore easier to manipulate^[7]. GO does not have a perfect honeycomb lattice, such as the one found on pristine graphene, it contains large amounts of defects which are advantageous since the electron transfer in sp^2 carbons occurs at the edges and in the aforementioned defects^[12]. The structure in GO is not fully planar due to the oxygen-containing groups in its damaged network, the atomically thin sheet of sp^2 carbon clusters is isolated by oxygenated sp^3 carbon domains. These groups can be beneficial to the further functionalization of the material. GO is nonconductive and photoluminescent over a broad spectrum, it is also an efficient fluorescence quencher making it an ideal choice for optical detection. GO can be reduced either chemically, thermally, electrochemically or photothermally. When

GO is reduced the sp^2 lattice is partially restored but it maintains some of the oxygen-containing groups. By controlling the amount of reduction it is possible to manipulate the optoelectronic properties in the material transforming it from an insulator to a semiconductor or even a semi-metal, and therefore obtain specific characteristics for specific uses^[14]. This tuning in electrical properties is especially useful in characterizing methods such as impedance spectroscopy (IS).

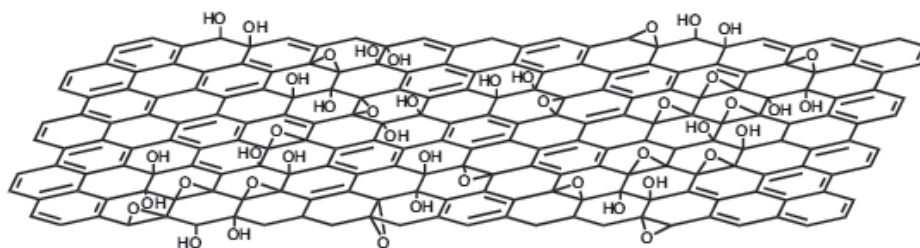


Fig. 1.5 Chemical structure of a single sheet of graphene oxide^[15].

1.3.2 Impedance spectroscopy (IS)

The introduction of electrochemical-based sensors has played a critical role in medical, clinical, environmental and industrial monitoring. The electrochemical sensors detect an electrical property such as resistance, current or potential and are classified depending on their measurement mode in potentiometric, conductometric or amperometric sensors. Information on various fundamental processes such as rate of ion exchange, charge transfer, diffusion, etc., can be obtained through IS^[31].

Impedance, though closely related to resistance, is however a complex value due to the change not only in amplitude but also in phase, giving more information on the performance of a given system. Impedance may be measured in time or frequency domain. For analysis in time domain a potential step function is applied to the system which results in a corresponding current time function. In the frequency domain a small excitation voltage is applied and the detected ac current is recorded, making it possible to determine the complex value shift, either in a Bode (modulus/phase) or a Nyquist plot (real/imaginary) (Fig.1.6). By making use of two closely spaced electrodes or IDEs it is possible to take advantage of the change in current flow occurring in the surface and therefore provide a high sensitivity against surface changes.

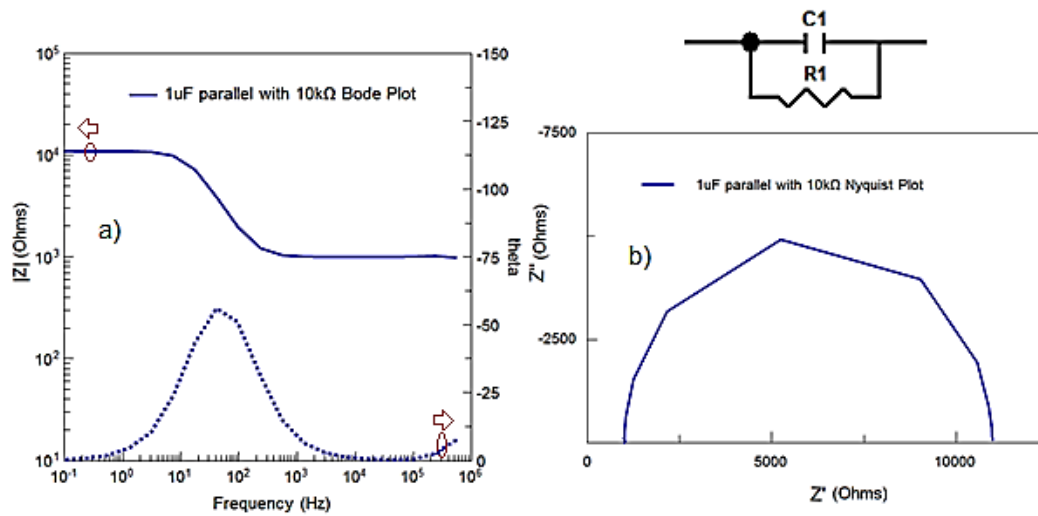


Fig 1.6. Impedimetric plots in a) Bode and b) Nyquist diagrams.

Impedance spectroscopy is useful in the monitoring of DNA hybridization because it is a label-free, direct method. A layer of ssDNA probe is immobilized on electrodes and will function as the recognition element in the sensor, while the electrodes act as the transducer. The two common ways to monitor the hybridization is either by oxidizing the DNA bases through a redox label or simply verifying the change in the resistance or capacitance of the surface before and after the event^[16].

1.3.3 Interdigitated electrodes (IDEs)

IDEs are a very attractive solution for impedimetric biosensing because they are highly tunable to the required specifications and furthermore they offer not only a sensing platform but an immobilization platform as well. After modification of the electrode with the recognition element it is possible to produce interfacial measurements. These measurements can involve the simple detection in the overall impedance at specific frequencies, but there is also the possibility to analyze the change in electrode capacitance^[16].

IDEs are normally considered lumped capacitors in order to simplify simulations. This assumption however, does not work at high frequencies. Each of the fingers has resistance and capacitance per unit length which constitute an RC network

with capacitance and resistance distributed along the fingers^[17]. Fig.1.7 shows the change in conditions on the sensor surface which enables the direct measurement of an electrical signal.

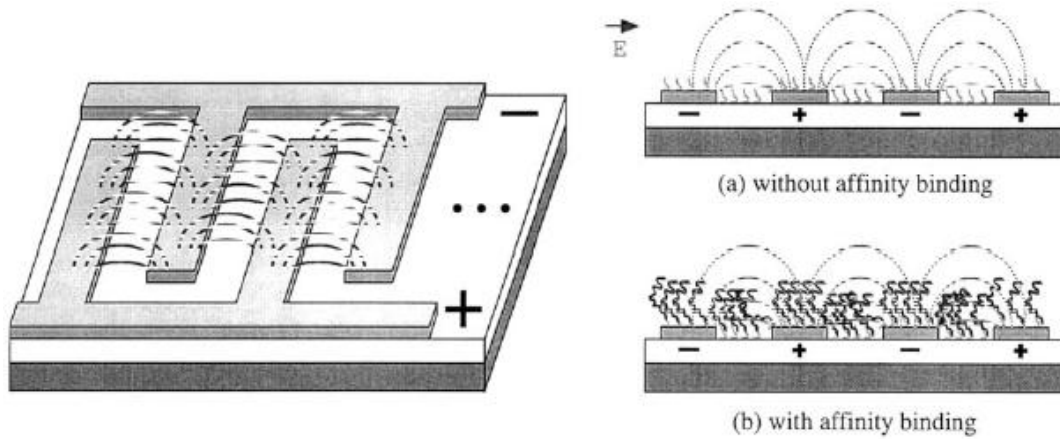


Fig.1.7 Principle of affinity binding of impedimetric sensor, a) without and; b) with molecules to be detected^[18].

It is not within the scope of this work to fully describe the design procedure for the IDEs used, the dimensions were however optimized before to ensure lower parasitic capacitances and smooth signal pathways. The size and spacing of the fingers was chosen in accordance to the fabrication capability of the optical lithography system at the clean room of the FH Kaiserslautern.

2. Materials and Methods

In this chapter the different materials, chemicals, equipment and protocols used in this research are discussed. Procedures that are systematic will only be mentioned in this chapter but a copy will be attached in the supplementary section of this work.

2.1 DNA sensor fabrication

2.1.1 Design of shadow mask for fabrication of IDEs

The IDEs mask consisted of arrays of 3 different sizes, the first array consisted of 340 fingers with $2.5\ \mu\text{m}$ width and inner spacing, 170 fingers with $5\ \mu\text{m}$ width and inner spacing, and finally 88 fingers with $10\ \mu\text{m}$ width and inner spacing, all three with a length of $1760\ \mu\text{m}$. The mask design was made with the Clewin 3.2.2 layout software (WieWeb software, the Netherlands).

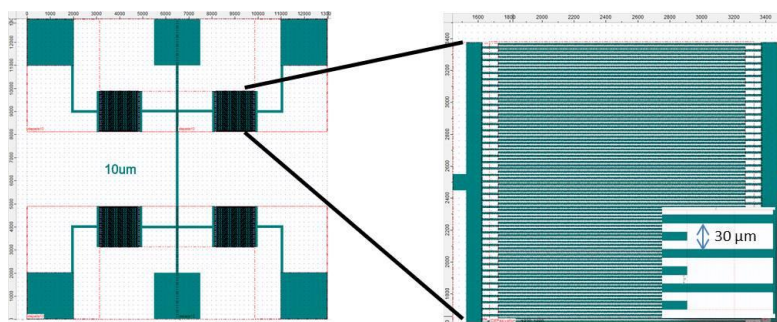


Fig.2.1 Design of the $10\ \mu\text{m}$ IDE mask using Clewin software.

The IDEs were fabricated on all wafers using standard photo lithography, using the protocol and facilities of Fachhochschule Kaiserslautern. The procedure schematics are shown on Fig 2.2, a complete description of the protocol will be added to the supplementary part of this work.

The first step is to spin coat the wafer with image reversal resist and apply the ultra violet (UV) light through the mask in order to activate the resist (a). The

wafer is then passed through the developer bench, spin dried and the structures have to be revised (b). The next step is the evaporation of the chrome-gold coating for the metallization (c). In order to achieve the lift-off the wafer is treated with acetone and washed with isopropanol (d). The wafer is again spin coated with resist in order to protect the structures during the cutting procedure (e). The wafer is cut, depending on the type of substrate and structure the procedure will have small variations such as the blade type (f).

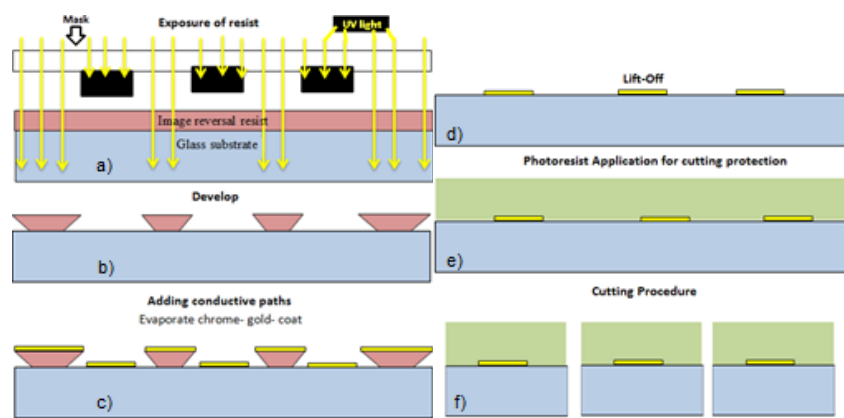


Fig.2.2 Fabrication process of the sensor chips (MContactPrintingSkript, S.Ingebrandt, FH Kaiserslautern).

2.1.2 GO deposition and dielectrophoresis (DEP)

In order to work with DEP a homogenous GO solution first had to be obtained. 25 mg of GO flakes (Graphene Supermarket) were sonicated in 250 ml of de-ionized (DI) water for 8 hours at maximum power (140%; Transsonic Digital ultrasonicator, T680 DH), every hour the solution was manually shaken in order to redisperse the larger flakes that had accumulated at the bottom of the bottle.

There are different methods to obtain graphene mono- and multilayers, which vary in several of the material's electrical properties such as electron mobility^[19]. It was decided to work with DEP due to it being a noninvasive, nondestructive method to manipulate particles, which has reported good results while working with single flakes of GO and even rGO^[20].

Electrokinetics comprehend the study of polarizable particle movement during interaction with a non-uniform ac electric field. DEP, an electrokinetic technique, specifically corresponds to the movement of these particles towards or away from strong electric field regions. By applying different voltages and frequencies along IDEs it is possible to move and position particles^[21].

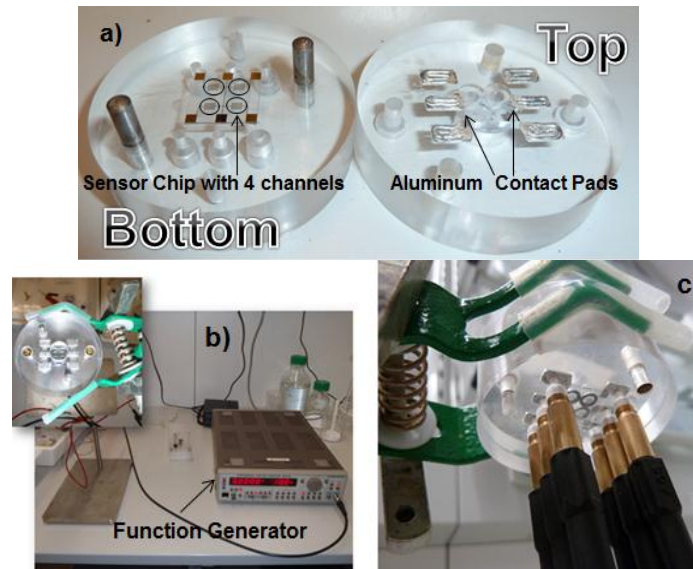


Fig. 2.3 Measurement cell and DEP setup; a) Open cell with the IDE chip, b) Function generator and top view of the cell where the GO is deposited, c) Bottom view of the connections for DEP.

The samples underwent a washing procedure with acetone, isopropanol and DI water in a 10 min ultrasonic bath each, followed by 1 min in a plasma oven at 140 W and 0.6 mbar oxygen to clean off remaining organic material and leave the surface hydrophilic for the even spread of the GO solution during DEP deposition. In the first experiments, the right settings for the deposition of GO on the Si/SiO₂ samples were determined. The Si/SiO₂ samples were chosen in order to see the coverage of the GO on an optical microscope. The parameters for DEP were based on Burg's work^[20] but just as he mentioned, it was noticed that the results varied drastically depending on the solution used. Using the measurement cell a 2.5 µl drop was applied on each of the four IDEs on the chip. The secondary electrodes in the chip were joined from the design, the primary electrodes however had to be wired in order to apply the signal simultaneously to all IDEs. After 15 minutes the signal was switched off and the chip was allowed to dry for 1 hour. The chip was then washed strongly with DI water. Excellent coverage on

75% of the samples was achieved. The starting parameters were 0.7 Volts peak (Vp) sinusoidal wave at a frequency of 10 MHz. The best results were obtained using a 5 Vp signal at 3 MHz. The next step was to deposit a homogenous layer of previously reduced GO on the IDEs. An HM 8130 function generator from Hameg (Livingston, Germany) was used in all DEP procedures.

2.1.3 Reduction of GO by L-Ascorbic acid (L-AA)

The most common chemical reduction is done with hydrazine or hydrazine hydrate^[22]. However, these chemicals are highly poisonous and explosive and furthermore not ecologically friendly. In this thesis a “green” approach based on reduction with L-AA^[23] was chosen. 50 mg of L-AA (Sigma Aldrich, Germany) on 5 ml of 0.1 mg/ml GO solution was used. After 24 hrs of constant stirring, the obtained solution changed color from light brown to black which is a visual effect of the reduction of GO.

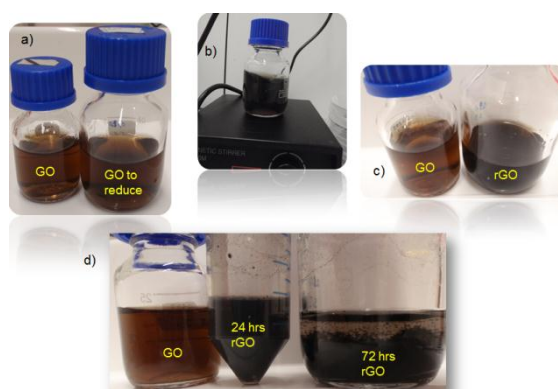


Fig.2.4. Different stages of GO reduction, a) GO solutions, b) GO solution during reduction, c) comparison of GO with 24 hrs rGO, d) GO vs. 24 and 72 hrs rGO.

The same protocol was followed as with the deposition of GO, however in this case the starting values consisted of 6 Vp at 1 MHz. The best results were achieved with 10 Vp at a frequency of 500 KHz. Using optical microscopy the coverage of the layer was verified and although the results were promising some aggregations of the flakes were observed in the rGO samples. It was therefore decided to reduce the layers after deposition. By leaving the samples for one week in a shaker with 4 ml of 30 mM L-AA ascorbic solution, the GO layers were successfully reduced after deposition, as well.

2.1.4 DNA Immobilization

Following the protocol from Bonanni et. al.^[24], 3 μ l of a 50 mM EDC and 30 mM sulfo-NHS solution was applied on each of the rGO covered IDEs in order to activate the carboxylic acid groups. After 1 hour the samples were washed with 1x PBS buffer, pH 7. The amino modified probe DNA was then applied to the IDEs in 3 μ l drops with a concentration of 1 μ M and left to incubate in a humidified environment overnight. As negative control fully mismatched (FMM) ssDNA was used on 2 IDEs and perfectly matched (PM) DNA was used on the remaining 2 (Fig.2.5). In order to remove nonspecifically adsorbed DNA and deactivate the remaining carboxylic groups from the samples, a washing step with 0.05% SDS and 40 mM hydroxylamine hydrochloride, nitrogen drying, a gentle rinse with DI water and finally nitrogen drying were used.

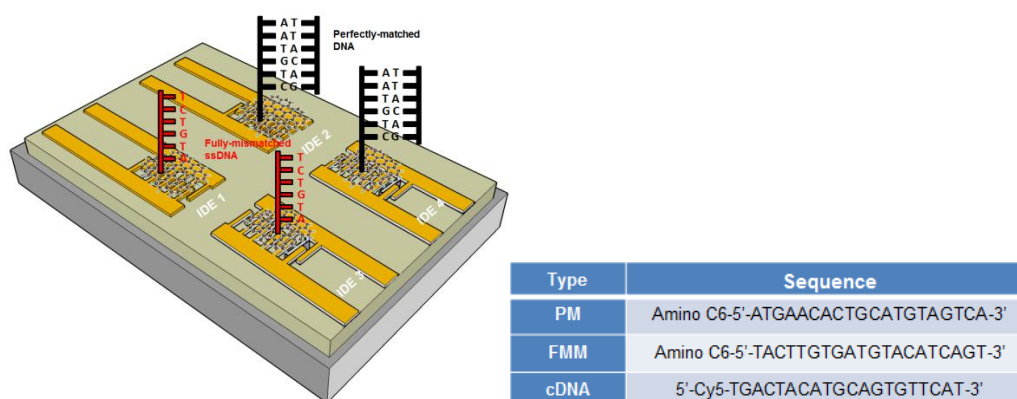


Fig.2.5 Schematic representation of the rGO functionalized IDEs DNA hybridization sensor and sequences of the used DNA. All DNA from Eurofins, Germany.

2.1.5 DNA Hybridization-Denaturation

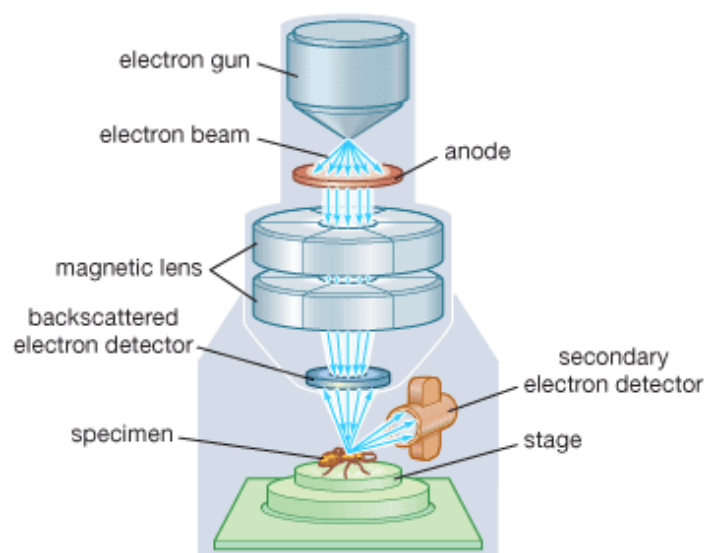
The fluorescent-labeled complementary DNA (cDNA) with a concentration of 5 μ M in TSC1 buffer (0.75 M NaCl, 75 mM trisodium citrate, pH 7) was heated up to 70°C and 3 μ l of this solution was applied to the IDEs and incubated for 1 hour at 42°C. The samples were finally washed two times with TSC2 buffer (0.30 M NaCl, 30 mM trisodium citrate, pH 7) followed by DI water. In order to obtain denaturation the samples were immersed in 0.1 M NaOH solution for 2 minutes and then washed thoroughly with DI water. All chemicals used from Sigma Aldrich and Merck, Germany.

2.3 Characterization

2.3.1 Scanning electron microscope (SEM)

In the SEM an accelerated beam of electrons is used on the sample. The energies may vary from hundreds to tens of thousands eV. The beam is localized upon the sample's surface and makes a scan following a parallel line path.

There are two fundamental types of radiation arising from this interaction, the secondary electrons and the backscattered electrons. The first consist of low energy electrons (tens of eV) which are emitted from the atoms closest to the surface after being struck by the electron beam. The backscattered electrons are the electrons coming from the electron beam after having interacted with the sample's atoms. The intensity of both emissions will vary depending on the angle between the beam and the materials surface, the topography and the chemical composition of the material under test. The emitted signal by the electrons and the radiation resulting from the impact is picked up by a detector and amplified in each position of the scan (Fig.2.6). When the sample is not a good conductor it is common to cover it with a metallic or carbon film to avoid it from getting charged^[25].



© 2008 Encyclopædia Britannica, Inc.

Fig.2.6 SEM basic setup.

2.3.2 Atomic force microscope (AFM)

The AFM scans a surface through a very small tip, only microns in length and even smaller in diameter, around 10 nanometers. The tip is set on a flexible bar or cantilever. This cantilever is bent when the tip contacts the sample. The bending of the cantilever is measured through a detector at the same time it scans the sample surface. The scanning can be done by moving the tip and leaving the sample static or vice versa. This type of microscope can be used on all kinds of samples, whether they are conductive, semiconductive or isolating.

There are several forces that act on the cantilever, one of them being the van-der-Waals force which can be attractive or repulsive depending on the distance between the atoms. This allows for two modes of operation: contact and noncontact mode. In the contact mode the cantilever is held a few Å above the surface and the interatomic force is repulsive. In the noncontact mode the cantilever is held tens of Å above the sample's surface and the forces are therefore attractive. In the so-called tapping mode, the cantilever is vibrated at its resonance frequency and the damping of the vibration due to the tip-surface interaction is extracted in a phase and an amplitude image.

Most AFM systems detect the position of the cantilever through optical means, usually a laser reflected on the cantilever which will act on a photodetector. The photodetector has partitions which allow the detection of small changes in the position of the incident beam, down to a few Å (Fig.2.7). Other purely electrical methods may be used assuming the cantilever is made from a piezoelectric material^[26].

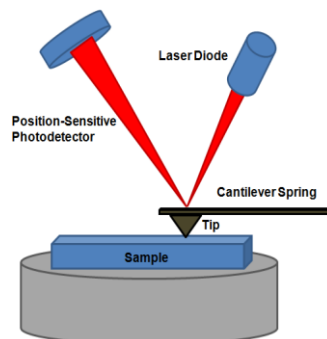


Fig.2.7 Basic AFM configuration.

3. Results and Discussion

In this chapter the different results obtained from the experiments and measurements will be presented and discussed.

3.1 GO solution

The first challenge came in obtaining a stable GO solution, and although in the published literature it sounded simple enough the results were not satisfactory until an ultrasonicator with enough power was used. The first ultrasonicator (Bandelin RK 100, Sonorex, Germany) worked at 35 kHz with 80 W of peak power and the solutions aggregated after a couple of days due to the big flakes in it, which for lack of power could not be broken down. After the change in ultrasonicator (Elma Transsonic Digitalis T680 DH, Germany) working at 40 kHz and 150 W of peak power the solution was stable for at least 3 months. The concentration of the GO in the solution also played an important part in the solution's stability and it was seen that with lower concentrations the stability in the obtained solution increased.

3.2 DEP deposition of GO and rGO

Different visual and electric techniques were employed for the characterization of the GO and rGO layers such as optical-, scanning electron-, atomic force microscopy and IS.

3.2.1 Physical characterization

It was earlier described that the force for DEP depends mainly on the polarizability of the particle and the electric field. The polarizability will depend on the type of particle and the frequency of the applied signal. The electric field on the other hand will depend on the geometry of the electrode array as well as the amplitude of the signal^[27].

Initial tests with DEP deposition revealed a voltage-frequency relation effect. If both values were chosen too high the gold in the IDEs peeled off. If the chosen values were too low the GO simply did not attach to the electrodes. Once the

right parameters were obtained on Si/SiO₂ samples as proven by optical microscopy (Fig.3.1), they were applied on the glass chips as well. This procedure had reproducible results, showing a well defined covering that ended abruptly on the borders of the IDEs showing different amount of layers as can be deduced from the different coloring^[10,28]. All optical microscope pictures were taken with an Olympus BX51 optical microscope (Olympus, UK).

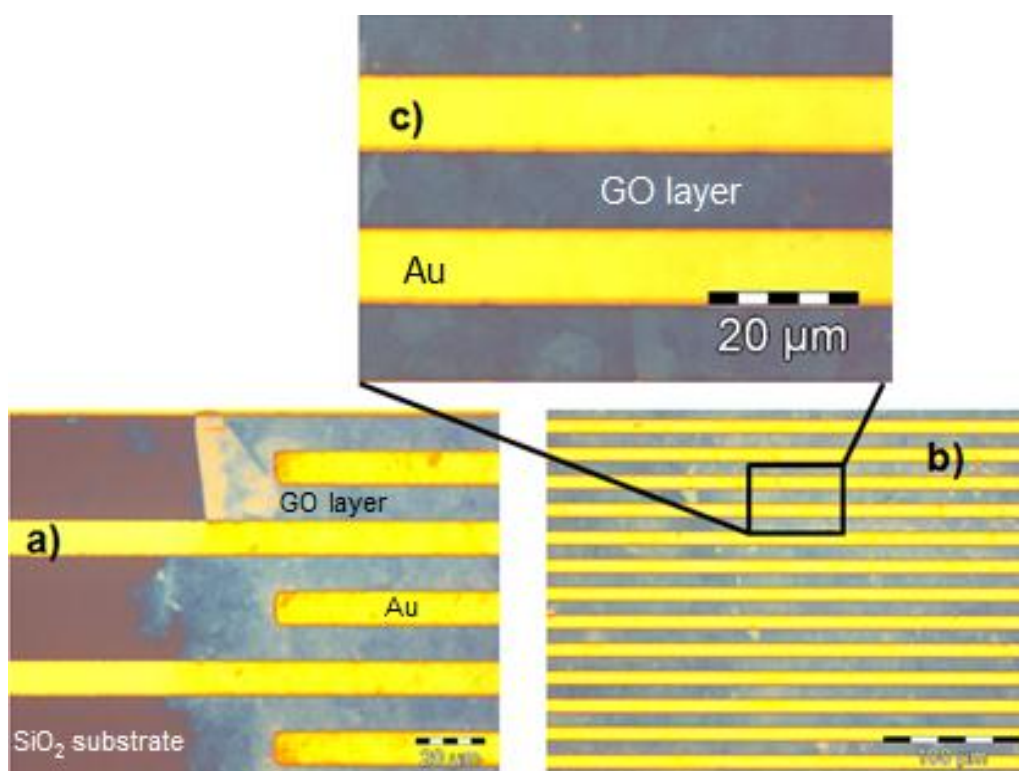


Fig.3.1 DEP deposition of GO on gold IDE with SiO₂ substrate, a) Limit of the layer determined by the IDE, b) Even covering of GO over the whole IDE, c) Close up on the GO layer.

The chemical reduction is speculated to proceed as two S_N2 nucleophilic reactions ending with a step of thermal elimination. Fig.3.2 represents the process in which L-AA makes the hydroxyls in GO more acidic through its electron-withdrawing five-membered ring, L-AA by dissociating two protons will function as a nucleophile. The two types of reactive species found in GO include epoxide and hydroxyl. The oxygen anion of L-AA, through a S_N2 nucleophilic attack, can open the epoxide. A back-side S_N2 nucleophilic attack may follow the reduction, releasing H₂O and forming an intermediate. The intermediate could be

eliminated thermally and thus rGO is formed. In the case of the hydroxyls, a double back-side S_N2 nucleophilic attack could displace them and the thermal elimination would reduce them further^[29].

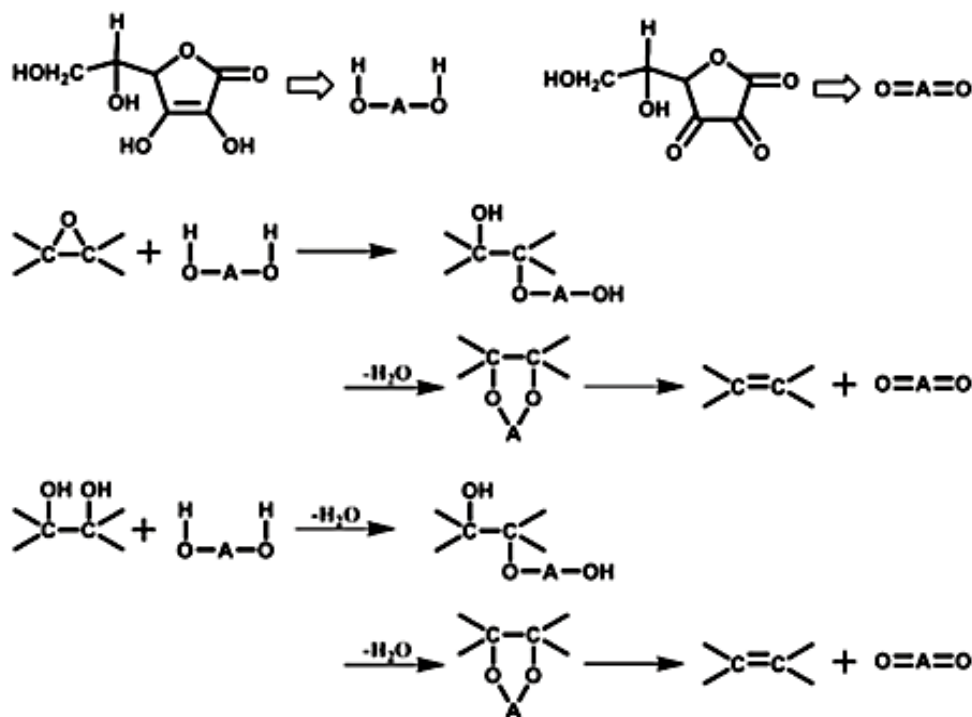


Fig.3.2 Proposed reaction pathway for the chemical reduction of graphite oxide with L-AA^[29].

The procedure with rGO began with the Si/SiO₂ samples and after several trials the desired results were reached. The technique was then used on the glass chips and although the outcome was not undesirable it was, however, harder to control. The different stages of reduction from the rGO solution played a major role in the deposition and therefore some aggregation of rGO flakes was seen on the IDEs (Fig.3.3).

Furthermore, it was only possible to work with the rGO solution for a day or it would continue to reduce even when taken off the stirrer, and finally aggregate irreversibly. It therefore became necessary to make a new solution every time rGO was needed for deposition, and in turn the resulting solution was not exactly the same.

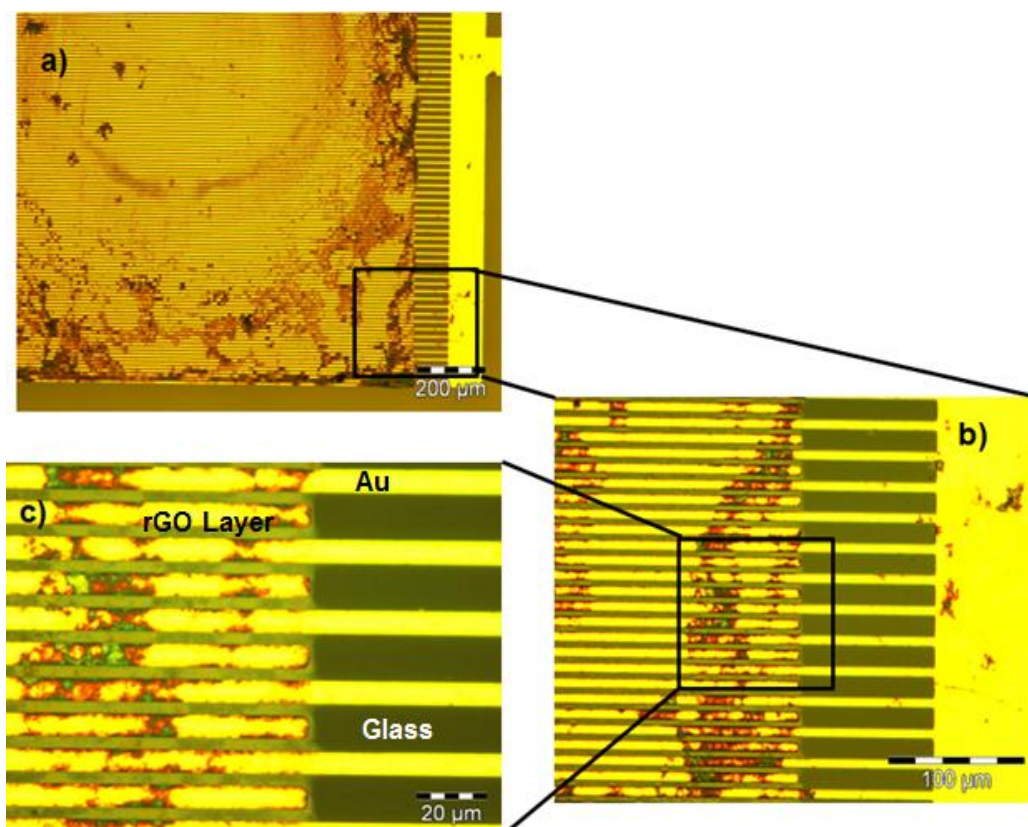


Fig.3.3 DEP deposition of rGO on gold IDEs with glass substrate, a) rGO aggregation on the IDE is visible, b) good delimitation of rGO covering c) Close up on the rGO layer.

Due to the fact that the GO solution deposition resulted in better reproducibility it was decided to reduce the GO layers after deposition. The GO deposition was stable and its stable attachment was verified after 4 days in PBS. On the other hand the GO-L-AA solution kept reducing even without stirring. Therefore, it was decided to place the GO covered IDEs in L-AA solution in a shaker. The results after seven days were visible to the naked eye and furthermore revised by SEM and AFM (Fig.3.4 and Fig.3.5).

In this case the sample was covered on the sides with silver paste to prevent it from getting charged. The SEM pictures corroborated the even distribution of the rGO and furthermore the specificity obtained from DEP as the layer was strictly contained within the boundaries of the IDE. The pictures also showed the ripples all along the layer which are characteristic of graphene. All SEM pictures were taken with a Zeiss Supra 40 SEM (Carl Zeiss AG, Germany).

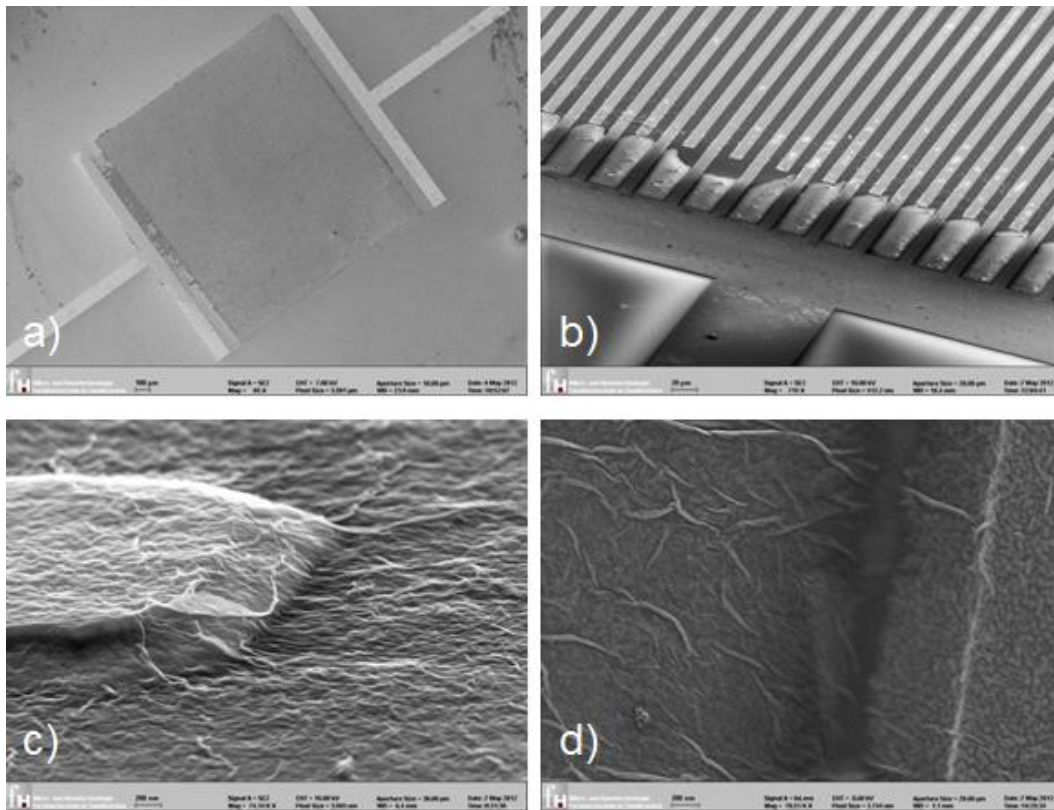


Fig.3.4 a) Complete IDE, b) Lateral view of the border of the IDE, c) Lateral view from an IDE finger, d) Top view from an IDE finger.

On subfigures b) to d) the scanning was performed with a tilting of the sample, which provided more information about the structure of the IDEs. The exact height was not possible to obtain with this method of characterization but the layer distribution and its surface between and over the IDEs is clearly visible. It was possible to observe (subfigure b)) some holes on the layer directly on top of the fingers. This effect was produced by the DEP deposition since the rGO flakes actually attempt to stay in between the fingers. However, due to the concentration of GO on the solution a semi-homogenous layer was formed which was suitable for the biosensor's purposes. On subfigure d) the structure of the gold finger under the layer can be seen.

For the AFM the sample needed no preparation except the manual focusing of the desired characterization area and the optimization of the scanning parameters. The AFM micrographs were able to give more information about the

height of the layer in the samples. Typically obtained thickness values were around 6 nm, which in turn means a 9 layer stacking of rGO flakes^[32]. All AFM pictures were taken using a NanoScope Dimension 3100 AFM (Veeco probes, USA).

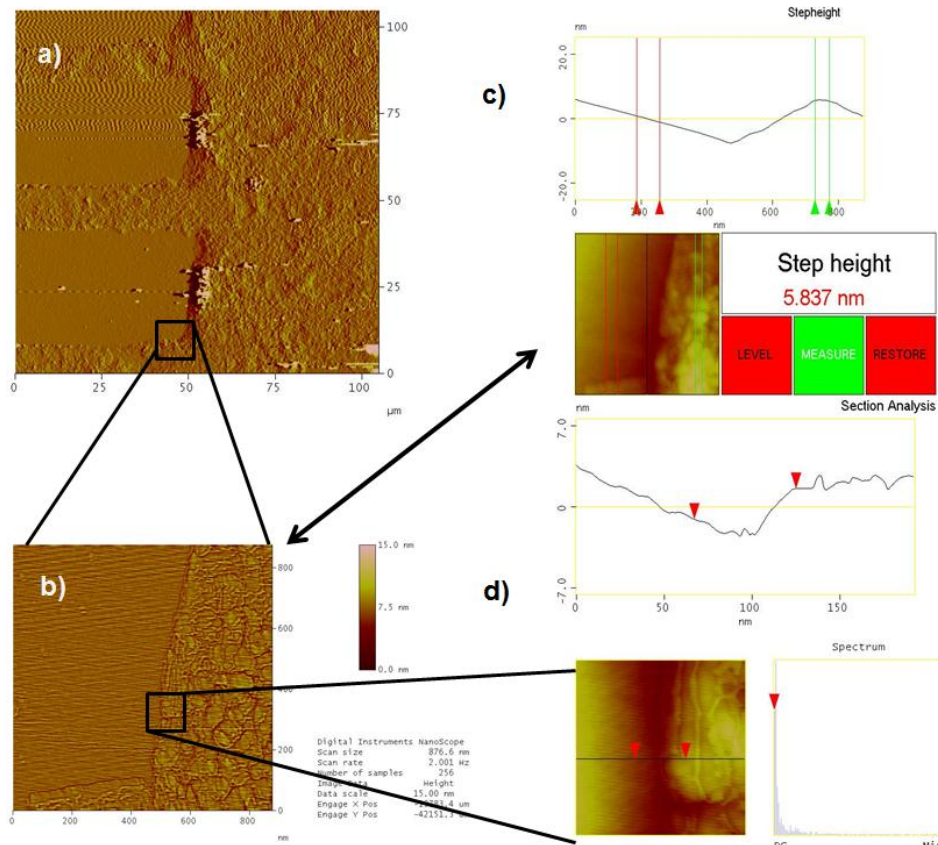


Fig.3.5 a) 100 μm area at the border between the glass substrate and the graphene layer; b) 800 nm close up of the border; c) step height of the 800 nm close up; d) 180 nm close up and section analysis of the area.

The different focus points on the figures gave an advantageous view of the height of the rGO layer. The different scans corroborated the smoothness in the layer and once again the feasibility of the deposition technique. This characterization was particularly important because the electrical properties of the biosensor depend strongly on the number of layers on top of the IDE. It has been reported that the increase in the number of layers will reduce the resistance of the whole sensor^[6]. However, by increasing the distance of the probe DNA from the gold IDEs the sensitivity is reduced.

3.2.2 Electrical characterization

Even though, the results varied considerably depending on the rGO solution used and therefore were not easily controllable or reproducible, the impedance measurements were a good electrical proof of the reduction. Not only did the impedance decrease visibly (several orders of magnitude in some cases), but the behavior of the system changed from capacitive to resistive as expected (Fig.3.6). All IS measurements were done using an Ivium Compactstat (Ivium Technologies, the Netherlands).

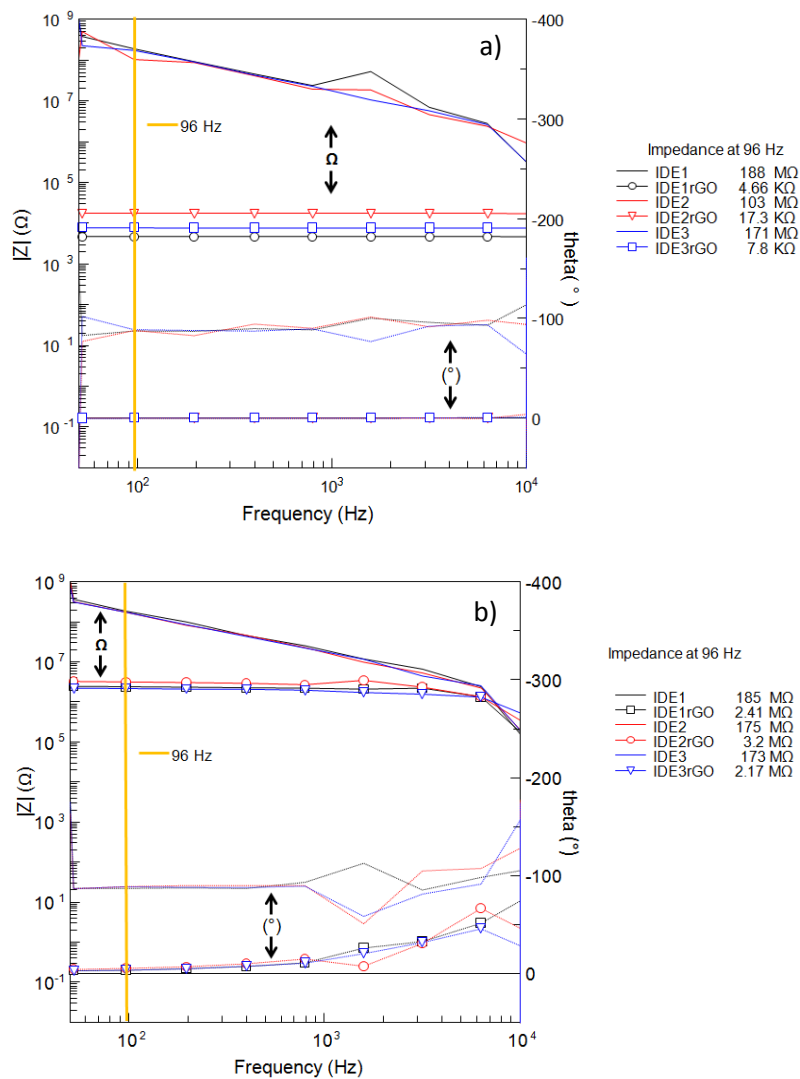


Fig.3.6 IS measurements of rGO on gold IDEs with glass substrate; a) Sample 1, b) Sample 2.

Results and discussion

The samples reduced after deposition also diminished their impedance and changed their behavior to resistive as their IS Bode and Nyquist diagrams show (Fig.3.7 and Fig.3.8). There were 61 frequency steps between 10 Hz and 10 MHz during the IS measurements.

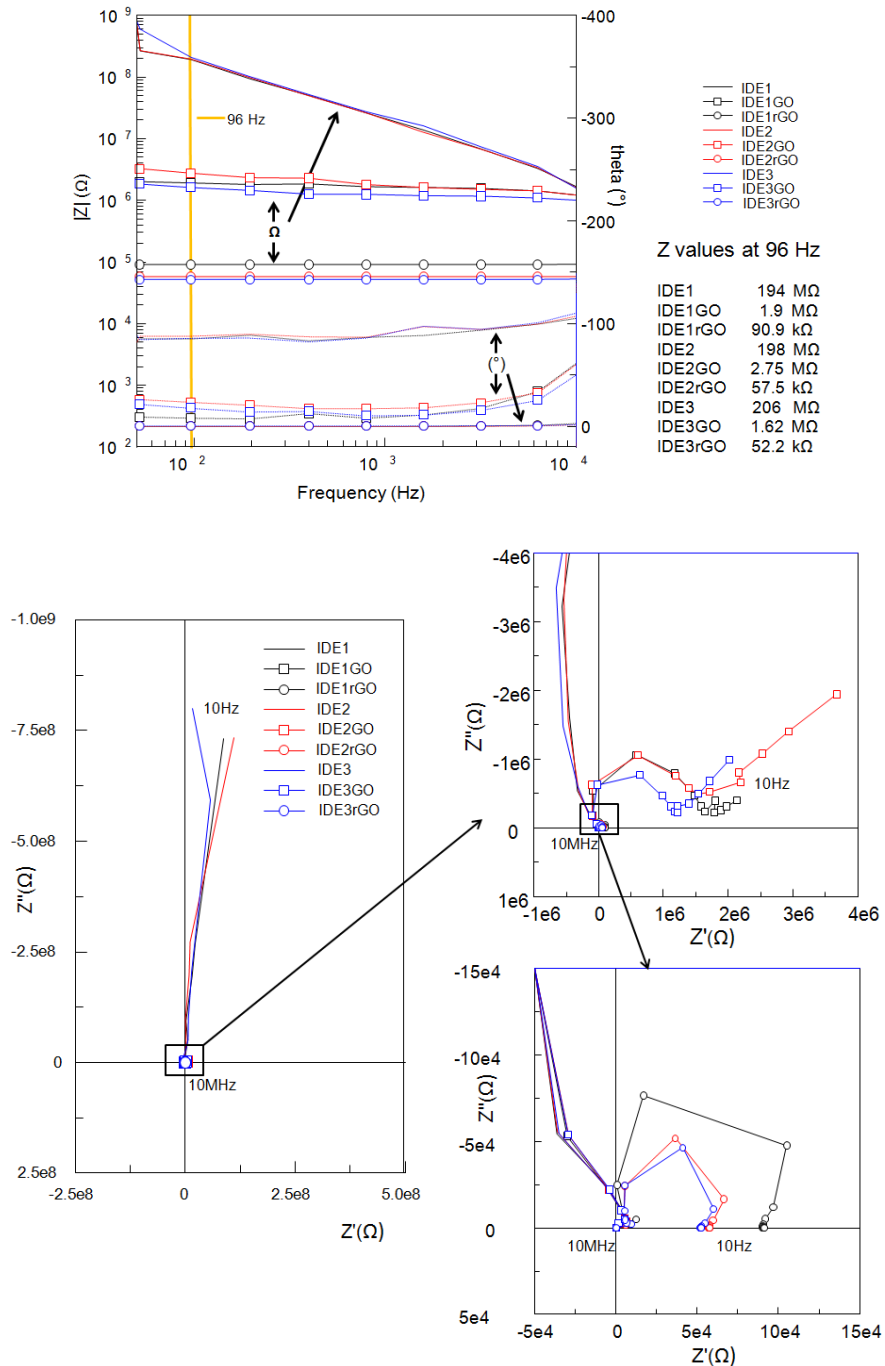


Fig.3.7 Bode and Nyquist plots of IS measurements from IDEs with glass substrate. First sample reduced after deposition of GO is shown.

Detection of DNA hybridization using IDEs functionalized with graphene

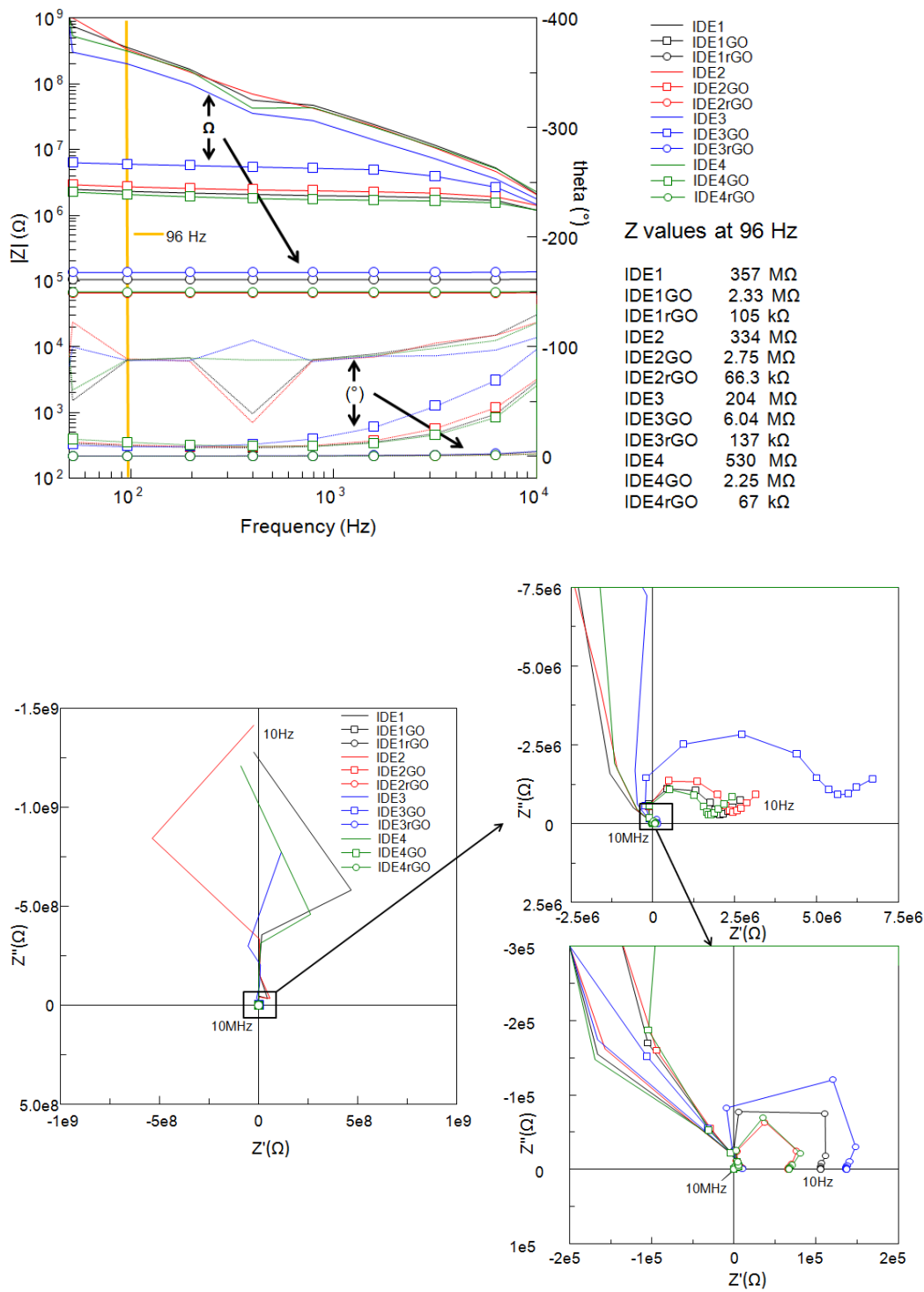


Fig.3.8 Bode and Nyquist plots of IS measurements from IDEs with glass substrate. Second sample reduced after deposition of GO is shown.

The homogeneity of the layer was already confirmed through physical characterization. The Nyquist and Bode plots, however, showed that the values

for GO deposition and subsequent reduction were better reproducible than the ones obtained with rGO solution. Furthermore, using the same solution without any degree of reduction made the experiments more repeatable.

3.3 DNA sensor

For DNA immobilization, hybridization and denaturation characterization fluorescence-scanning microscopy and IS were used.

3.3.1 Physical characterization

The DNA molecules were labeled with Cy5 fluorescence dye. Unfortunately the standard Cy5 filter in the microscope setting was not available. Therefore it was necessary to use a Typhoon Trio fluorescent scanner (GE Healthcare, United States). The results can clearly be compared before and after denaturation as shown on Figure 3.9. The size of each square's side is 2 mm.

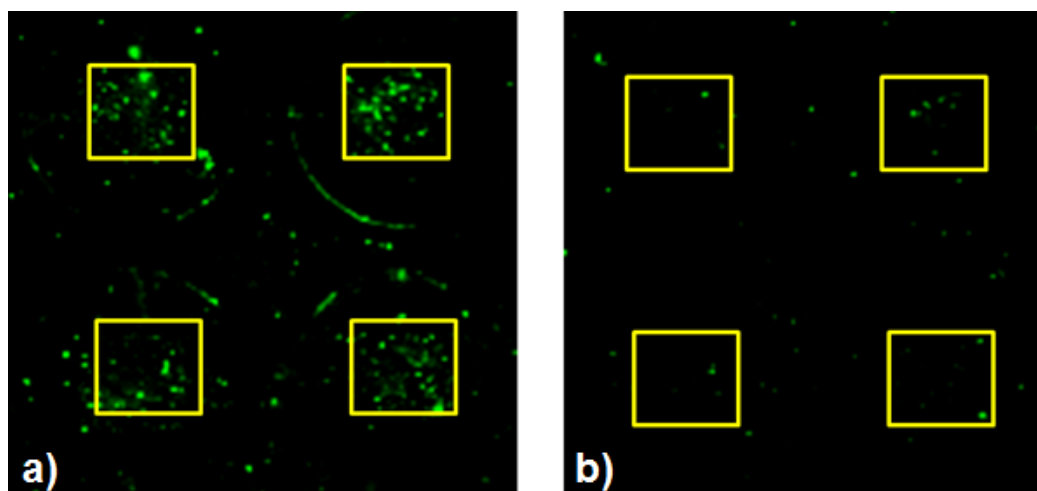


Figure 3.9 Scanning fluorescence pictures before (a) and after denaturation (b).

3.3.2 Electrical characterization

The Bonanni et. al. protocol used^[24] turned out to produce samples of high quality. The results obtained from the immobilization, hybridization and denaturation were very satisfactory. The used covalent method with EDC chemistry for immobilization (Fig.3.10) provided very reproducible data.

Detection of DNA hybridization using IDEs functionalized with graphene

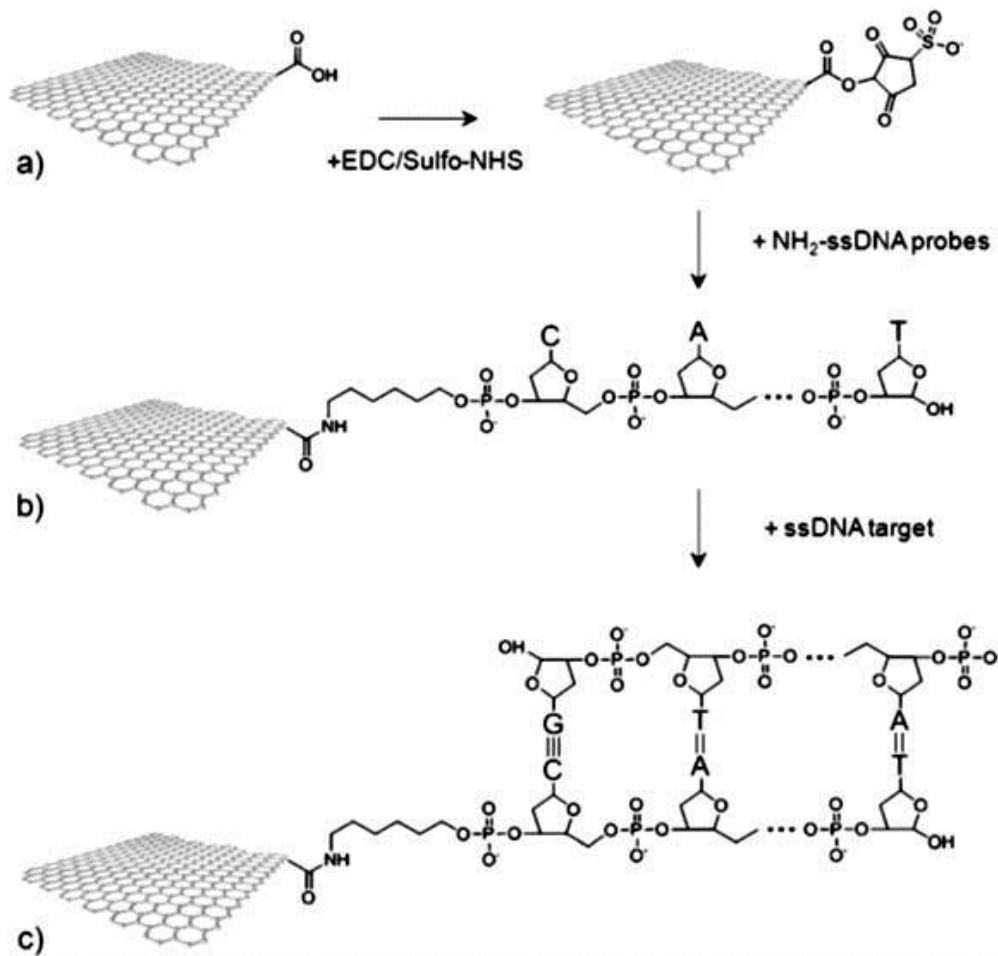


Fig.3.10 EDC chemistry used for covalent functionalization of ssDNA on graphene, a) An amide bond is formed by the reaction of sulfo-NHS esters with the amino modified ssDNA probes, b) ssDNA covalently functionalized graphene, c) Hybridization after incubation with cDNA^[24].

As a first experiment only perfectly-matched ssDNA probe was used in 7 samples. 6 out of the 7 first samples produced good results (Fig.3.11). Perfectly-matched and fully mismatched DNA was later used in order to obtain a negative control. 5 out of the 7 samples provided good results (Fig.3.12).

Results and discussion

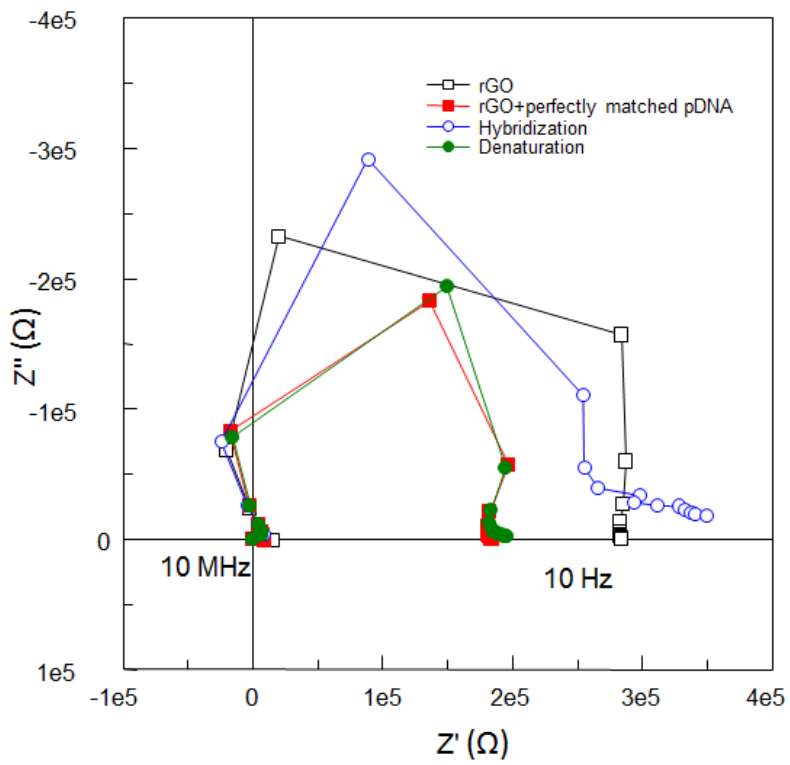
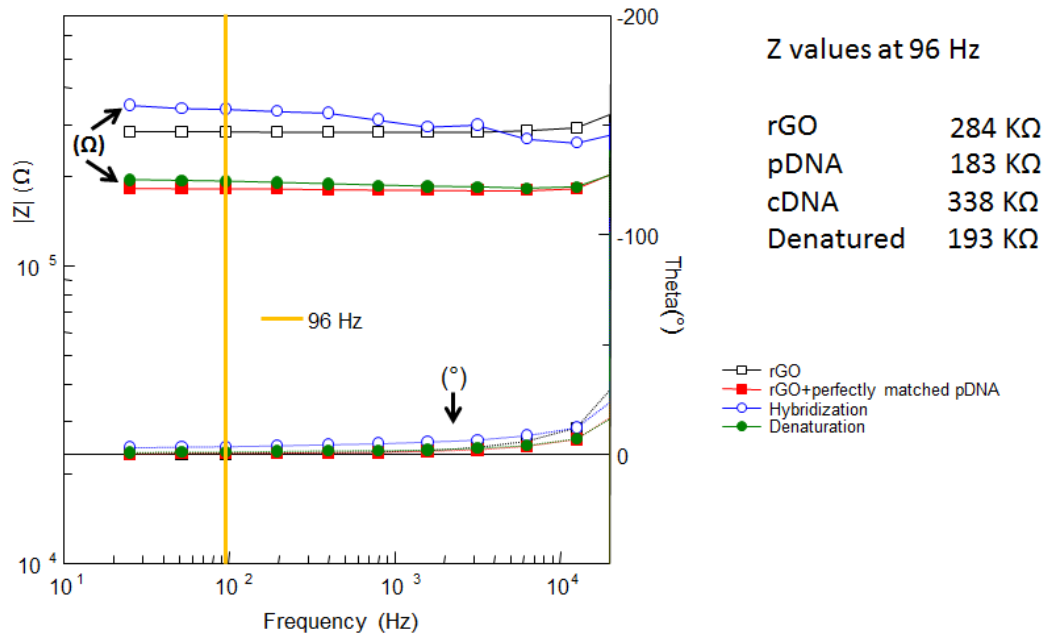


Fig. 3.11 Bode and Nyquist plots of perfectly matched DNA immobilization, hybridization and denaturation.

Detection of DNA hybridization using IDEs functionalized with graphene

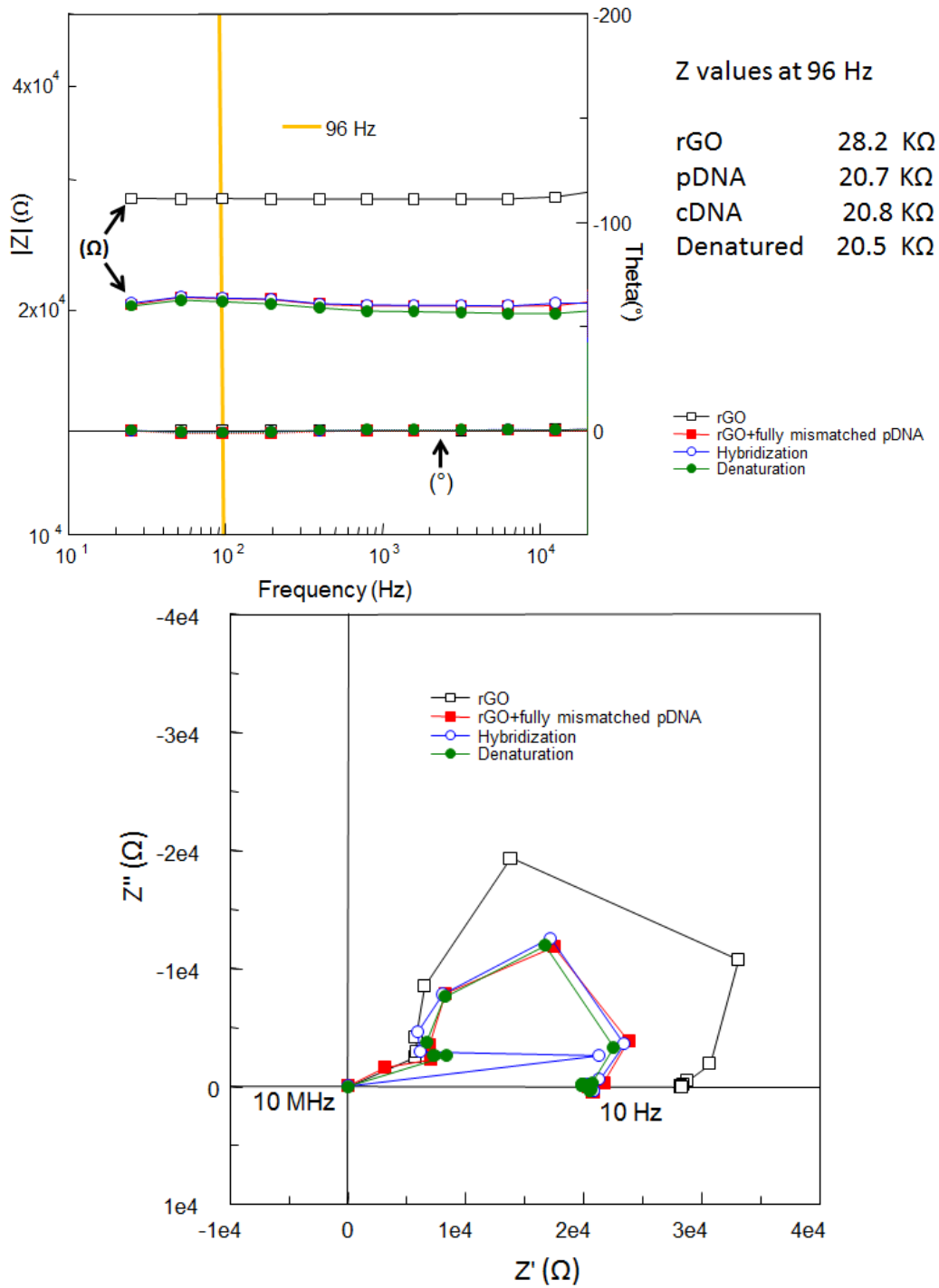


Fig. 3.12 Bode and Nyquist plots of fully mismatched DNA immobilization, hybridization and denaturation.

The rest of the graphs can be observed in the supplementary section. It is noteworthy to list the extracted values at 96 Hz, however. A nice reproducibility in the experiments was achieved. After immobilization the impedance of the

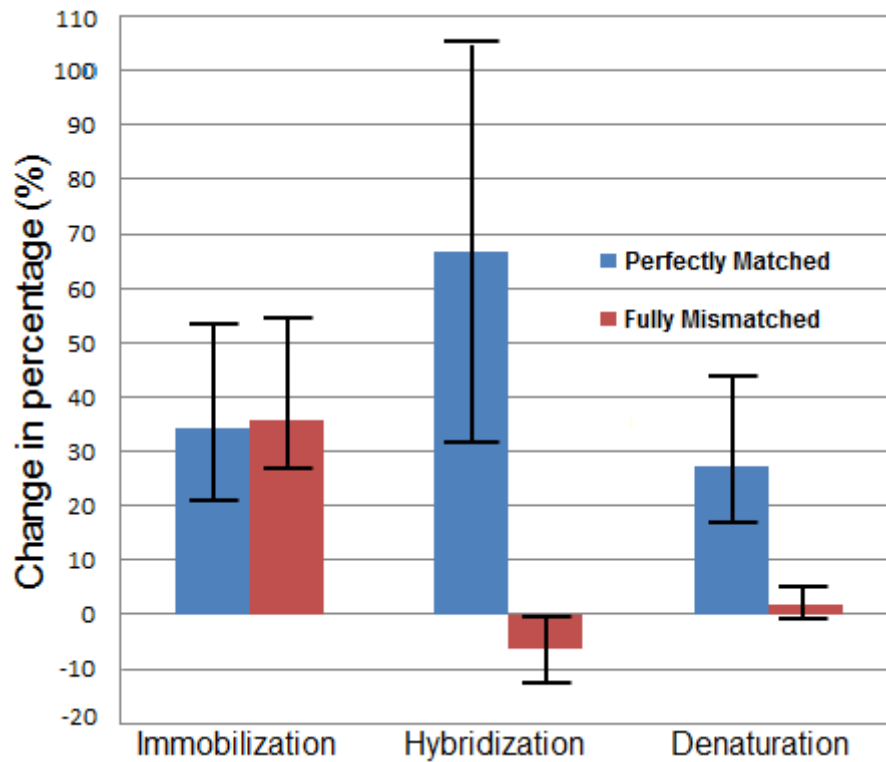
Results and discussion

sensors decreased probably due to the paths created around the rGO defects by the ssDNA molecules. During hybridization an increase of impedance was observed. In denaturation the expected reduction in impedance was obtained, returning to the immobilization parameters (Table 3.1).

Table 3.1 Results of IS measurements of perfectly matched and fully mismatched DNA strands after GO reduction, immobilization, hybridization and denaturation. Values at 96 Hz were extracted from the impedance spectra.

Type of Sample	Z(Ω) rGO	Z(Ω) after Im.	Z(Ω) after Hy.	Z(Ω) after De.
1st Sample pM	57.16 K	45.4 K	73.62 K	60 K
2nd Sample pM	37.46 K	29.4 K	46.75 K	39 K
3rd Sample pM	5.8 M	2.31 M	6.53 M	2.9 M
4th Sample pM	670 K	313 K	560 K	411 K
5th Sample pM	284 K	184 K	360 K	196 K
6th Sample pM	612 K	335 K	687 K	421 K
7th Sample pM	446 K	344 K	463 K	353 K
8th Sample pM	87.5 K	52.24 K	68.2 K	53.13 K
1st Sample fM	114 K	53.41 K	45.35 K	45.67 K
2nd Sample fM	28.2 K	20.7 K	20.8 K	20.6 K
3rd Sample fM	21.2 K	15.31 K	14.73 K	13.89 K

Although the individual readings of the impedance values were different from sensor to sensor, the changes in the different samples were related to the amount of GO and the reduction on them. Therefore a change in percentage could be made. Results of all experiments are summarized in graph 3.1.



Graph 3.1 Changes in the percentage of the impedance values for the different DNA experiments extracted from the impedance spectra at 96 Hz.

Due to the relative changes in the initial values of the different samples, further experiments are needed in order to obtain a more accurate quantification of the response of the sensor. Nonetheless, even in the cases of smallest change a 16.5% could be recorded, and the average change even after taking the greatest value off the chart was still over 30%. The results are given as mean +/- standard deviation from 10 individual experiments.

4. Conclusions and outlook

Plenty of insight into the behavior and the handling of GO was gained. Starting from the original GO solution, the impact of different concentrations and ultrasonication power on the final size of the flakes was verified, and therefore the stability of the solutions was thoroughly investigated. As different approaches with the L-AA reduction were tried, the effects of the stirring speed, ratio of L-AA to GO and time on the reduction were verified. It was even possible to continue the reduction of a sample when the measured impedance was not satisfactory. It was not possible to verify the limit of reduction by Raman spectroscopy due to time constraints. However, further experiments will be undertaken, which will accomplish the tuning in the reduction of the solution to fit specific needs.

The chosen protocol of deposition, DEP, also proved to be highly efficient and furthermore extremely stable as it was proven by the samples left for 7 days in a shaker with L-AA solution. It was possible to observe how the reduction process actually removed some layers of graphene through the mechanical shaking, therefore giving a smaller number of rGO layers on the final samples and thus getting closer to the sought after monolayer. A lower limit determination on the concentration in the GO solution will be the next step in order to reduce the number of layers on the samples starting from the deposition step. It is expected that by tuning the solution concentration and the parameters on the electrical signal applied during DEP, a GO monolayer could be formed on the sensor and therefore increase its sensitivity.

The chosen protocol for DNA immobilization and hybridization produced extremely repeatable results. There is still a need, however, to tune the different aspects such as ssDNA concentrations, incubation times and temperatures, etc. in order to proceed from simple hybridization detection further to single nucleotide polymorphism detection capabilities.

The original scope of this thesis was completely fulfilled, however. A sensor for DNA hybridization with IDEs functionalized with graphene was fabricated. All the techniques and methods to achieve this goal were realized with basic research

Conclusions and outlook

equipment and what is more important using a “green” approach. To our knowledge this is the first time a combination of IDEs and DEP was used to form a layer of GO on top of the IDEs. A new “shaking” technique was developed as a variation to the L-AA reduction to obtain a DNA hybridization sensor.

The integration of graphene into biosensing will prove to be a major advantage scientifically and economically to whoever achieves it first in a commercial way. Even though due to time constraints it was not possible to optimize the different protocols or even test for single nucleotide polymorphisms, the results obtained in this thesis are very promising. The procedures chosen for the different steps of the sensor fabrication are not only highly tunable and repeatable but above all in complete agreement of what the green technology science is demanding nowadays. Improvement in the different steps of the protocols will be included in following works.

References

- [1] A. Barth, W. Marx, *Graphene - A rising star in view of scientometrics* **2008**, <http://arxiv.org/ftp/arxiv/papers/0808/0808.3320.pdf>.
- [2] Virendra Singh, Daeha Joung, Lei Zhai, Soumen Das, Saiful I. Khondaker, Sudipta Seal, *Progress in Materials Science* **2011**, *56*, 1178.
- [3] K. Bourzac, *Nature* **2012**, *483*, S34.
- [4] C. Schmidt, *Nature* **2012**, *483*, S37.
- [5] N. Savage, *Nature* **2012**, *483*, S38.
- [6] R. Ruoff, *Nature* **2012**, *483*, S42.
- [7] M. Pumera, *Materials Today* **2011**, *14*, 308.
- [8] A. Bonanni, M. Pumera, *ACS Nano* **2011**, *5*, 2356.
- [9] Y. Shao, J. Wang, H. Wu, J. Liu, I. A. Aksay, Y. Lin, *Electroanalysis* **2010**, *22*, 1027-1036.
- [10] K. Wang, J. Ruan, H. Song, J. Zhang, Y. Wo, S. Guo, D. Cui, *Nanoscale Res Lett* **2010**.
- [11] Z. Yin, Q. He, X. Huang, J. Zhang, S. Wu, P. Chen, G. Lu, Q. Zhang, Q. Yan, H. Zhang, *Nanoscale* **2011**, *4*, 293.
- [12] Y. Liu, X. Dong, P. Chen, *Chem. Soc. Rev* **2012**, *41*, 2283.
- [13] T. Jacobs, *Nanostructures as platform for biosensors.*, Diepenbeek, Belgium **2011**.
- [14] Caterina Soldano, Ather Mahmood, Erik Dujardin, *Carbon* **2010**, *48*, 2127.
- [15] K. P. Loh, Q. Bao, G. Eda, M. Chhowalla, *Nature Chem* **2010**, *2*, 1015.
- [16] O. Pänke, T. Balkenhohl, J. Kafka, D. Schäfer, F. Lisdat, in *Biosensing for the 21st Century*, Vol. 109 (Eds.: R. Renneberg, F. Lisdat), Springer Berlin / Heidelberg **2008**, p. 195.
- [17] C. Chung, S. Smith, A. Menachery, P. Bagnaninchi, A. J. Walton, R. Pethig, in *2011 IEEE ICMTS International Conference on Microelectronic Test Structures*, IEEE **2011**, p. 74.
- [18] Peter Van Gerwen, Wim Laureyn, Wim Laureys, Guido Huyberechts, Maaik Op De Beeck, Kris Baert, Jan Suls, Willy Sansen, P. Jacobs, Lou Hermans, Robert Mertens, *Sensors and Actuators B: Chemical* **1998**, *49*, 73.

References

- [19] C. N. R. Rao, K. S. Subrahmanyam, H. S. S. Ramakrishna Matte, B. Abdulhakeem, A. Govindaraj, B. Das, P. Kumar, A. Ghosh, D. J. Late, *Sci. Technol. Adv. Mater* **2010**, *11*, 54502.
- [20] B. R. Burg, *Directing Carbon Nanotubes and Graphene: Fundamentals and Parallel Device Integration using Dielectrophoresis*, Zurich **2010**.
- [21] H. Morgan, A. G. Izquierdo, D. Bakewell, N. G. Green, A. Ramos, *J. Phys. D: Appl. Phys* **2001**, *34*, 1553.
- [22] D. R. Dreyer, S. Park, C. W. Bielawski, R. S. Ruoff, *Chem. Soc. Rev* **2010**, *39*, 228.
- [23] J. Zhang, H. Yang, G. Shen, P. Cheng, J. Zhang, S. Guo, *Chem. Commun* **2010**, *46*, 1112.
- [24] A. Bonanni, A. Ambrosi, M. Pumera, *Chemistry – A European Journal* **2012**, *18*, 1668-1673.
- [25] L. E. S. Soares, L. R. Cortez, R. O. de Zarur, A. A. Martin, *Microsc Microanal* **2012**, *18*, 289.
- [26] H. X. You, L. Yu, *Methods in Cell Science* **1999**, *21*, 1.
- [27] A. Kuzyk, *ELECTROPHORESIS* **2011**, *32*, 2307-2313.
- [28] I. Jung, J.-S. Rhyee, J. Y. Son, R. S. Ruoff, K.-Y. Rhee, *Nanotechnology* **2012**, *23*, 25708.
- [29] J. Gao, F. Liu, Y. Liu, N. Ma, Z. Wang, X. Zhang, *Chem. Mater* **2010**, *22*, 2213.
- [30] B. van Grinsven, N. Vanden Bon, L. Grieten, M. Murib, S. D. Janssens, K. Haenen, E. Schneider, S. Ingebrandt, M. J. Schöning, V. Vermeeren, M. Ameloot, L. Michiels, R. Thoelen, W. de Ceuninck, P. Wagner, *Lab Chip* **2011**, *11*, 1656.
- [31] B. Pejčić, R. de Marco, *Electrochimica Acta* **2006**, *51*, 6217.
- [32] I. K. Moon, J. Lee, R. S. Ruoff, H. Lee, *Nat Comms* **2010**, *1*, 1.

Supplementary Section

Part 1: IS measurements

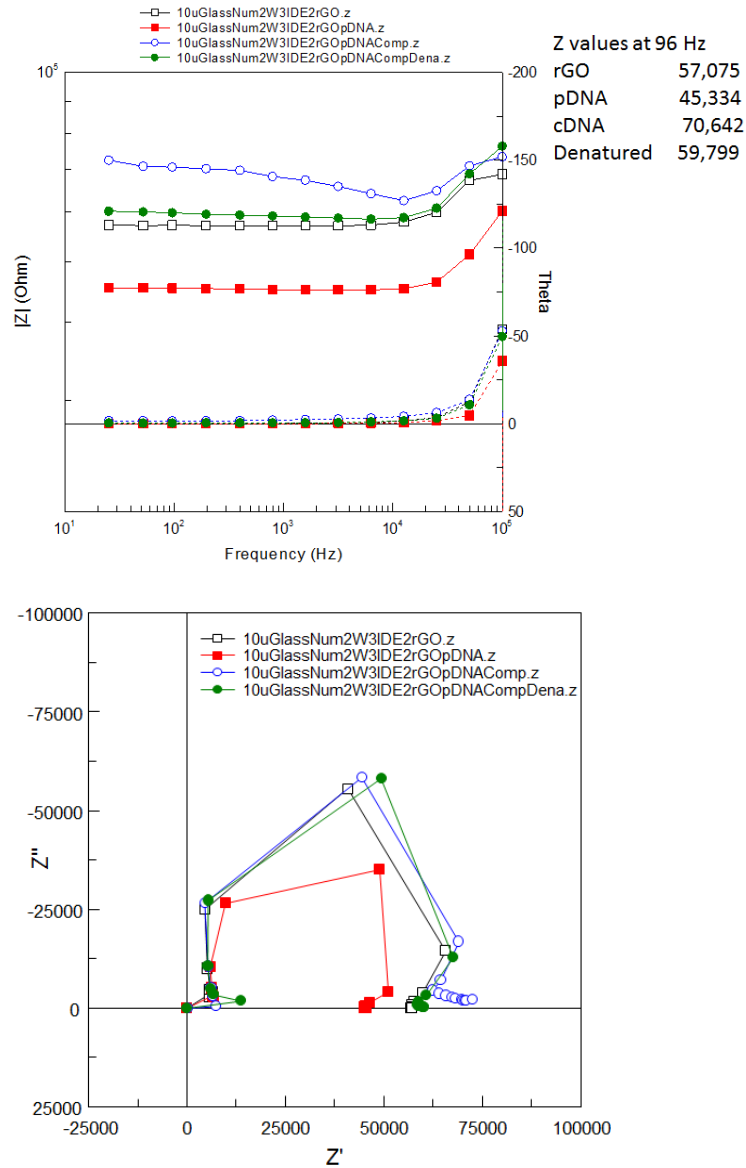


Fig. 1.1 Bode and Nyquist plots of perfectly matched DNA immobilization, hybridization and denaturation.

Supplementary section

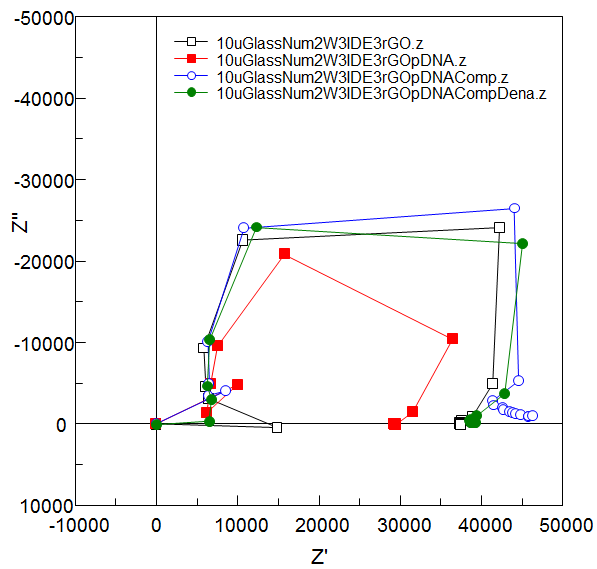
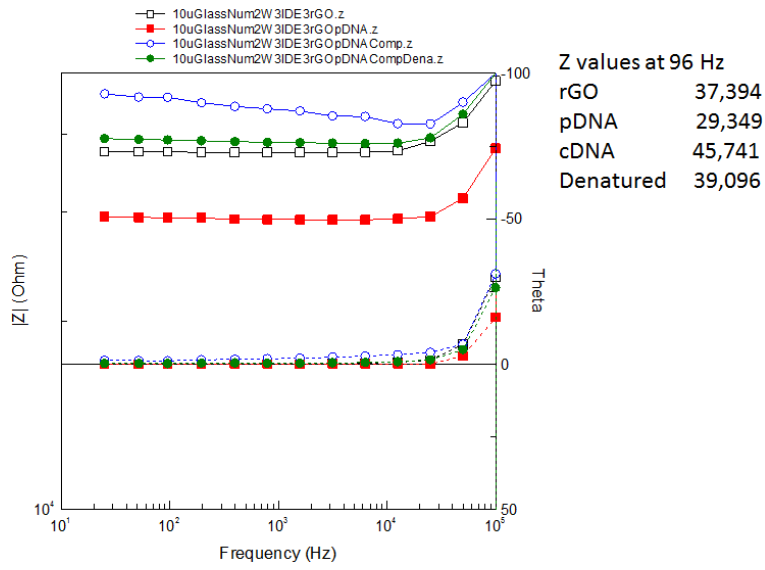


Fig. 1.2 Bode and Nyquist plots of perfectly matched DNA immobilization, hybridization and denaturation.

Detection of DNA hybridization using IDEs functionalized with graphene

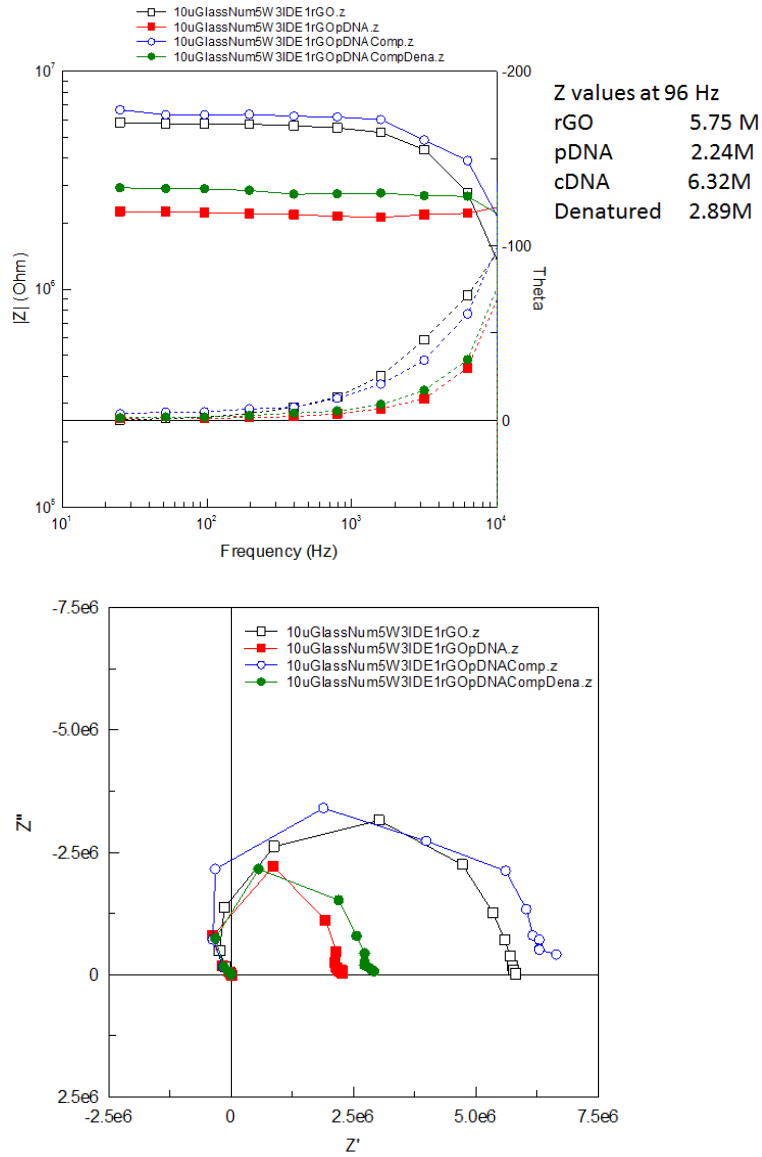


Fig. 1.3 Bode and Nyquist plots of perfectly matched DNA immobilization, hybridization and denaturation.

Supplementary section

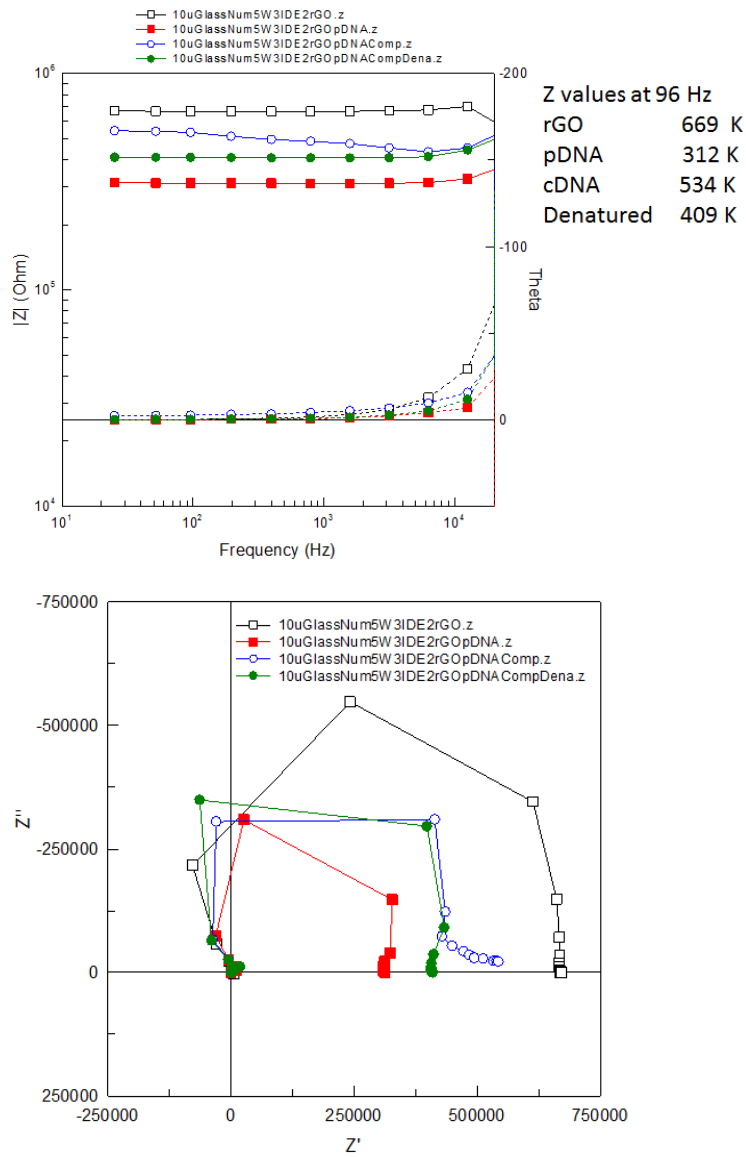


Fig. 1.4 Bode and Nyquist plots of perfectly matched DNA immobilization, hybridization and denaturation.

Detection of DNA hybridization using IDEs functionalized with graphene

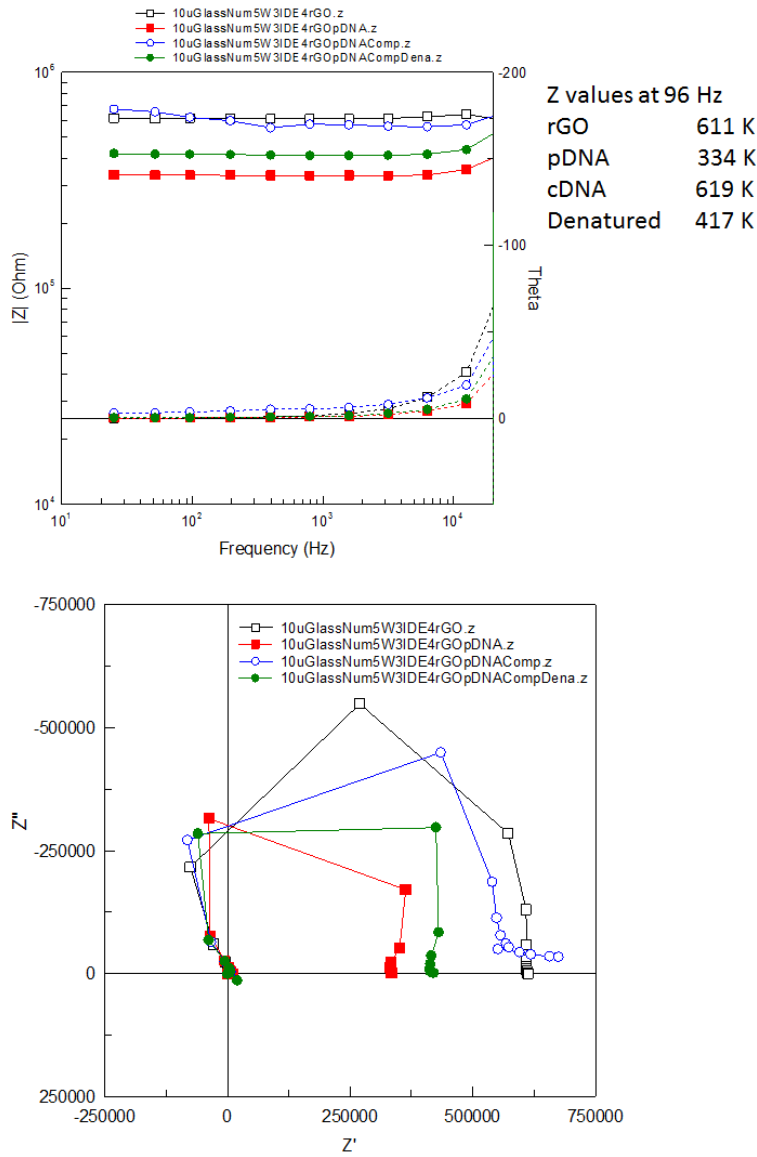


Fig. 1.5 Bode and Nyquist plots of perfectly matched DNA immobilization, hybridization and denaturation.

Supplementary section

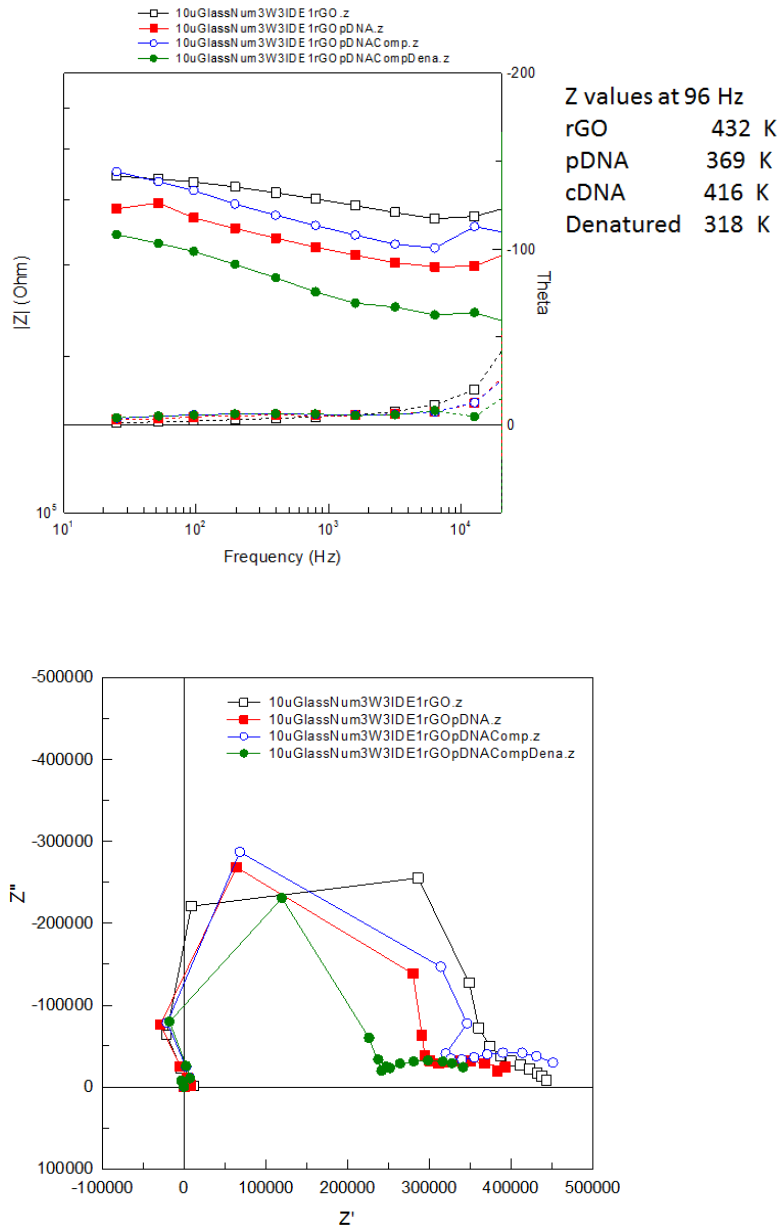


Fig. 1.6 Bode and Nyquist plots of perfectly matched DNA immobilization, hybridization and denaturation.

Detection of DNA hybridization using IDEs functionalized with graphene

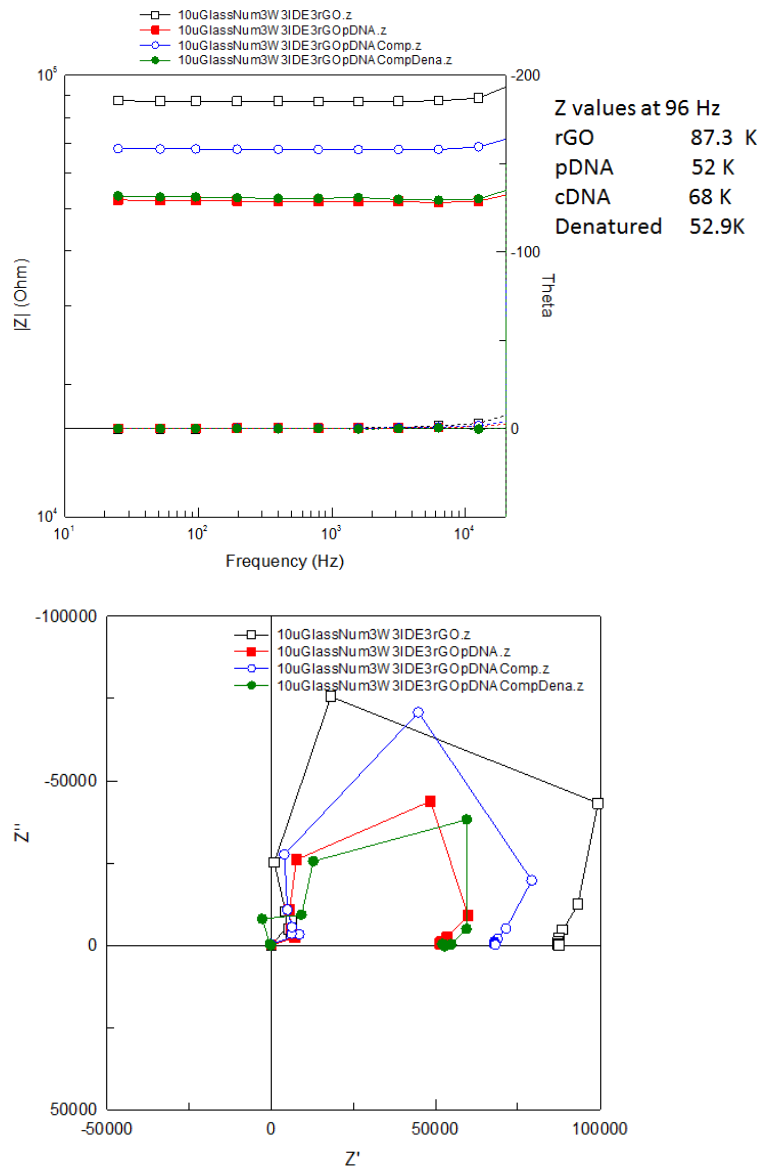


Fig. 1.7 Bode and Nyquist plots of perfectly matched DNA immobilization, hybridization and denaturation.

Supplementary section

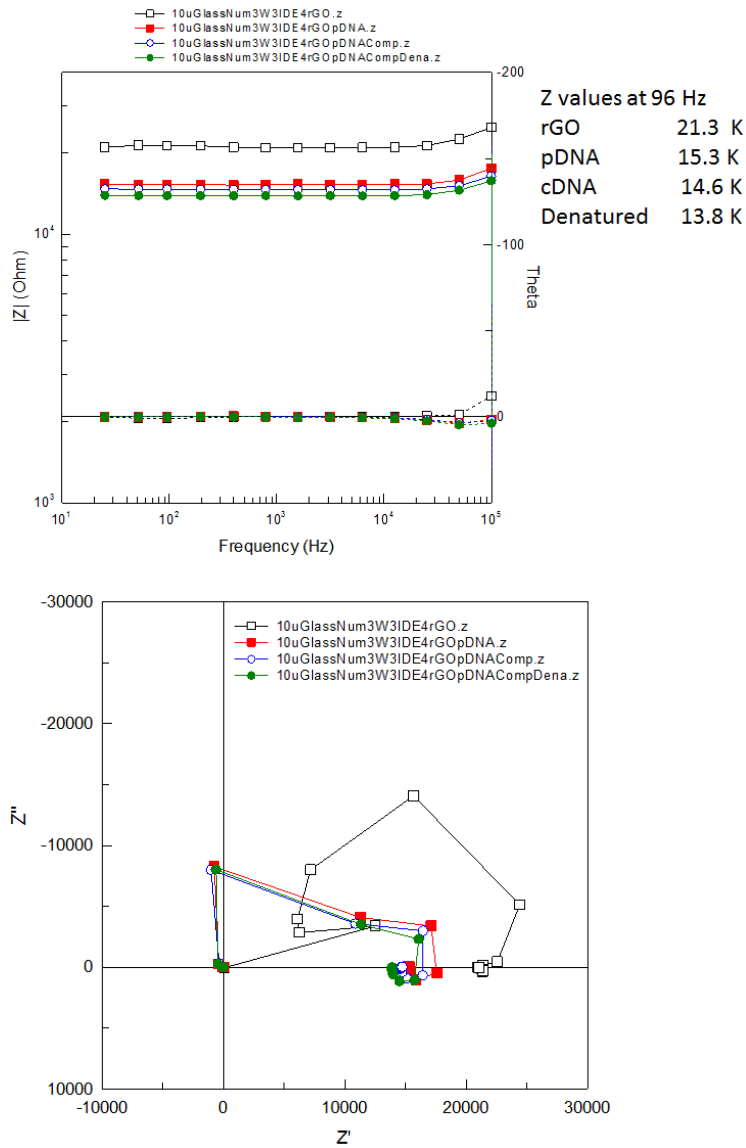


Fig. 1.8 Bode and Nyquist plots of fully mismatched DNA immobilization, hybridization and denaturation.

Detection of DNA hybridization using IDEs functionalized with graphene

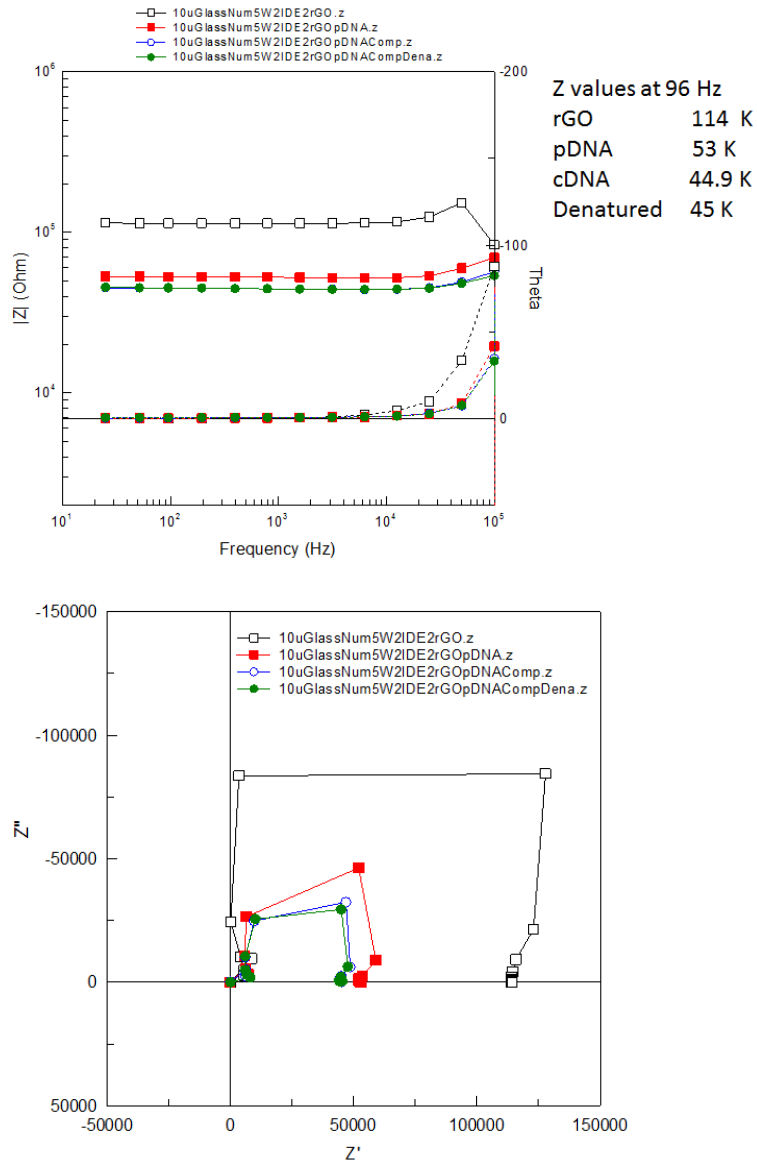


Fig. 1.9 Bode and Nyquist plots of fully mismatched DNA immobilization, hybridization and denaturation.

Part 2: Chip fabrication protocol

Cleaning Wafer

Step	System / Process	Material	Data
1	SRD	DI	Progr. 1 700rpm, 3min; DI; 2000rpm; 4min; N2
2	Sulfuric Acid	H2SO4 95%; H2O2 30%	115°C; 10min; ca. 20-40ml H2O2 dose in basin
3	QDR (Quick Dump Rinser)	DI	2 – 3min
4	SRD	DI	Progr. 1 700rpm, 3min; DI; 2000rpm; 4min; N2
5	Plasma stripper	O2	40% O2; 350W, 5min

Lithography of conducting paths

Step	System / Process	Material	Data
6	Hotplate		180° C, 10min 10 min cooling
7	SpinCoater BLE	AR-U 4030	Prog.: BLE \ Rezepte \ Lacke \ AR-U-4030.txt 4ml / 7sec, 500rpm; 60sec, 2000rpm
8		Hotplate Lanz	Prog.: AR4030 85°C; 2min
9		10min cooling	
10	MA/BA6	Mask 1	10sec; 6mW; vacuum contact Mode

Detection of DNA hybridization using IDEs functionalized with graphene

11	Hotplate BLE Süss		115°C; 5min
12		10min cooling	
13	MA/BA6	Flood exposure	25sec; 6mW
14	Developer bench	AR 300-26; DI	1:3; ca. 15sec.
15	Spin-dryer	Progr. 1 3000rpm, 30sec	
16	Microscope	Structure control	

Metallization

Step	System/ Process	Material	Data
17	Plasma stripper	O ₂	40% O ₂ ; minimal power 250 Watt, 36 sec
18	Evaporation	Cr, Au	Progr. MEA_Chrom 30-3000nm Cr: 100Å, 2Å/s, power 47%, Progr. Cr_Boat1-MEA_1.bot Au: 3000Å, 5Å/s, power 51%, Progr. Au_Tiegel4-MEA_1.ebg

Lift off

Step	System / Process	Material	Data
19	US basin	Acetone glass1 Acetone glass2	5min; 60W 1min; new Acetone
20	Cleaning bench	Isopropanol	Washing up
21	QDR	DI	2min
22	SRD	DI	Progr. 1 700rpm, 3min; DI; 2000rpm; 4min; N ₂

Wafer cutting

Step	System	Material	Data
23	SpinCoater BLE	AR-U 4030	5ml; 3000rpm; 60sec
24	Hotplate BLE		87°C; 5 min
25		10min cooling	
26		Adhesive foil	
27	Wafer-sawing	GA 851-xxx	5mm/s y1= 40mm; y2= 39mm; z1=80µm; z7=2mm
28	Cleaning bench	Acetone; DI; Isopro.	Stripping

Part 3: Measurement cell design

The measurement cells were produced in the workshop of the FH KI.

Lower part - mechanical drawing

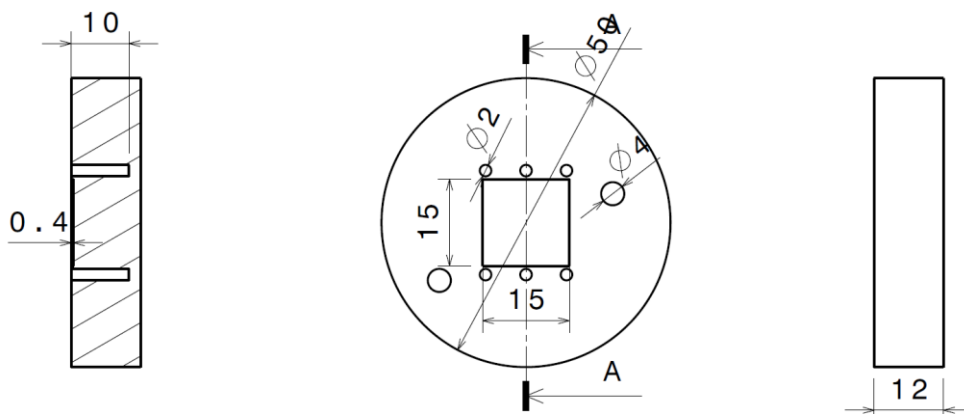


Figure 1: Design of measurement cell (lower part)

Cut A-A

front view

side view

1:1 scale

1:1 scale

1:1 scale

Upper part – mechanical drawing

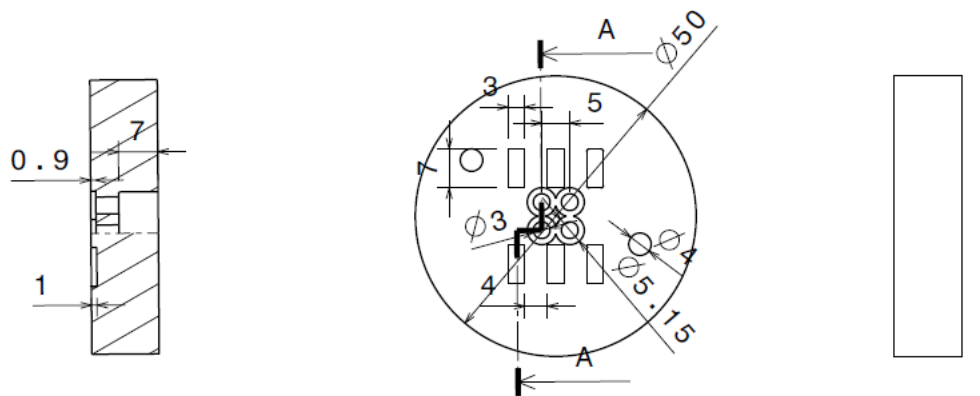


Figure 2: Design of measurement cell (upper part)

Cut A-A

front view

side view

1:1 scale

1:1 scale

1:1 scale

Auteursrechtelijke overeenkomst

Ik/wij verlenen het wereldwijde auteursrecht voor de ingediende eindverhandeling:

Detection of DNA-Hybridization Using Interdigitated Electrodes Functionalized with Graphene

Richting: **master in de biomedische wetenschappen-bio-elektronica en nanotechnologie**

Jaar: **2012**

in alle mogelijke mediaformaten, - bestaande en in de toekomst te ontwikkelen - , aan de Universiteit Hasselt.

Niet tegenstaand deze toekenning van het auteursrecht aan de Universiteit Hasselt behoud ik als auteur het recht om de eindverhandeling, - in zijn geheel of gedeeltelijk -, vrij te reproduceren, (her)publiceren of distribueren zonder de toelating te moeten verkrijgen van de Universiteit Hasselt.

Ik bevestig dat de eindverhandeling mijn origineel werk is, en dat ik het recht heb om de rechten te verlenen die in deze overeenkomst worden beschreven. Ik verklaar tevens dat de eindverhandeling, naar mijn weten, het auteursrecht van anderen niet overtreedt.

Ik verklaar tevens dat ik voor het materiaal in de eindverhandeling dat beschermd wordt door het auteursrecht, de nodige toelatingen heb verkregen zodat ik deze ook aan de Universiteit Hasselt kan overdragen en dat dit duidelijk in de tekst en inhoud van de eindverhandeling werd genotificeerd.

Universiteit Hasselt zal mij als auteur(s) van de eindverhandeling identificeren en zal geen wijzigingen aanbrengen aan de eindverhandeling, uitgezonderd deze toegelaten door deze overeenkomst.

Voor akkoord,

Lanche, Ruben

Datum: **13/06/2012**